Published in final edited form as:
J Med Chem. 2014 August 14; 57(15): 6751–6764. doi:10.1021/jm500791c.

A Novel Class of Bis- and Tris-Chelate Diam(m)inebis(dicarboxylato)platinum(IV) Complexes as Potential Anticancer Prodrugs

Hristo P. Varbanov[*,†], **Simone Göschl**[†], **Petra Heffeter**[‡,§], **Sarah Theiner**[†,§], **Alexander Roller**[†], **Frank Jensen**[‖], **Michael A. Jakupec**[†,§], **Walter Berger**[‡,§], **Markus Galanski**[*,†], and **Bernhard K. Keppler**[†,§]

[†]Institute of Inorganic Chemistry, University of Vienna, Waehringer Strasse 42, 1090 Vienna, Austria

[‡]Comprehensive Cancer Center and Department of Medicine I, Institute of Cancer Research, Medical University of Vienna, Borschkegasse 8a, 1090 Vienna, Austria

[§]Research Platform “Translational Cancer Therapy Research”, University of Vienna, Waehringer Strasse 42, 1090 Vienna, Austria

[‖]Department of Chemistry, University of Aarhus, Langelandgade 140, 8000 Aarhus C, Denmark

Abstract

A novel class of platinum(IV) complexes of the type [Pt(Am)-($R(COO)_2)_2$], where Am is a chelating diamine or two monodentate am(m)ine ligands and $R(COO)_2$ is a chelating dicarboxylato moiety, was synthesized. For this purpose, the reaction between the corresponding tetrahydroxidoplatinum(IV) precursors and various dicarboxylic acids, such as oxalic, malonic, 3-methylmalonic, and cyclobutanedicarboxylic acid, was utilized. All new compounds were characterized in detail, using 1D and 2D NMR techniques, ESI-MS, FTIR spectroscopy, elemental analysis, TGA, and X-ray diffraction. Their in vitro cytotoxicity was determined in a panel of human tumor cell lines (CH1, SW480 and A549) by means of the MTT colorimetric assay. Furthermore, the lipophilicity and redox properties of the novel complexes were evaluated in order to better understand their pharmacological behavior. The most promising drug candidate, **4b** (Pt(DACH)$(mal)_2$), demonstrated low in vivo toxicity but profound anticancer activity against both the L1210 leukemia and CT-26 colon carcinoma models.

[*]**Corresponding Authors**: (H.P.V.) Phone: +43-1-4277-52662. Fax: +43-1-4277-52680. hristo.varbanov@univie.ac.at.; (M.G.) Phone: +43-1-4277-52600. Fax: +43-1-4277-52680. markus.galanski@univie.ac.at.

ASSOCIATED CONTENT

Supporting Information

TG/DTA curves of compound **1b**; $^{1}H^{13}C$ HMBC spectra of complex **5b*** after addition of ascorbate; proposed reduction pathway of novel platinum(IV) complexes; platinum accumulation in mouse tissues, blood, and urine after treatment with **4b**; ^{195}Pt and ^{15}N NMR chemical shifts of novel complexes; structure refinement details for **1c** and **4a**; elemental analysis data; and X-ray crystallographic data in CIF format. This material is available free of charge via the Internet at http://pubs.acs.org. Crystallographic data have been deposited with the Cambridge Crystallographic Data Center under nos. CCDC 1001737 and 1001738. Copies of the data can be obtained, free of charge, on application to CCDC, 12 Union Road, Cambridge CB2 1EZ, UK (deposit@ccdc.com.ac.uk).

The authors declare no competing financial interest.

Europe PMC Funders Author Manuscripts

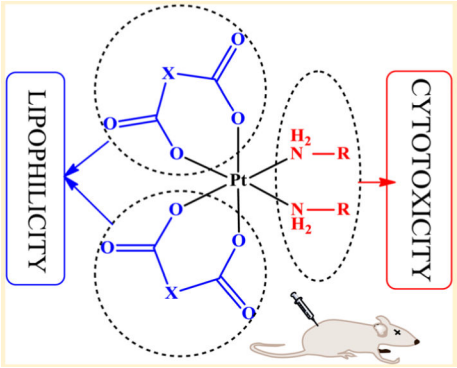

INTRODUCTION

Platinum(II)-based cytotoxic agents, namely, cisplatin, carboplatin, and oxaliplatin (Scheme 1), are a part of more than 50% of clinically applied anticancer regimens, and first-line chemotherapy for 12 neoplasms includes platinum drugs.[1,2] Their clinical effectiveness is, however, accompanied by severe dose-limiting side effects, acquired and/or intrinsic tumor resistance, and the inconvenient and cost-intensive parenteral administration.[3,4]

Platinum(IV) complexes are promising candidates as novel chemotherapeutics capable of overcoming several problems associated with existing platinum(II)-based anticancer therapy. Their physicochemical properties, retained cytotoxicity, and diverse possibilities for derivatization offer a variety of opportunities for the development of an effective and safe platinum prodrug for oral application.[3,5-10] Therefore, hundreds of Pt(IV) compounds have been synthesized, their biological activity has been evaluated, and three complexes (tetraplatin, iproplatin, and satraplatin) have been examined in clinical trials. However, there is still no platinum(IV) complex approved for clinical use.[1] Clinical studies with satraplatin are ongoing, while the status of its adamantylamine analogue, LA-12, in clinical development is unclear.[1,11]

Platinum(IV) complexes are considered to be prodrugs which have to be activated in vivo by reduction, followed by aquation of the formed Pt(II) species prior to interaction with nuclear DNA.[3,6,12,13] The low anticancer activity and/or high general toxicity often observed for highly cytotoxic platinum-(IV) compounds is usually related to poor pharmacokinetics, due to rapid and premature reduction in vivo.[14,15] Consequently, selection of a suitable ligand sphere to assure appropriate kinetics of activation is essential for the clinical success of platinum(IV) anticancer prodrugs. In line with these requirements, *cis,cis,trans*-diam(m)inedichloridodicarboxylato-platinum(IV) complexes feature such a favorable coordination sphere, which is believed to be optimal.[3,6,16] However, it was recently shown that these types of complexes can also be rapidly reduced in vivo and deactivated before reaching the tumor.[15,17,18] Therefore, there is still need for the design of novel platinum(IV) compounds that have alternative ligand spheres and offer improved pharmacokinetic behavior. Current efforts have been directed toward the development of platinum(IV) complexes containing two different axial ligands on the same scaffold, revealing some advantages in terms of solubility, lipophilicity, redox behavior, and targeting strategies.[19-23]

In the present article, we report on the synthesis and characterization of a series of novel platinum(IV) complexes with a ligand sphere based on two chelating dicarboxylato ligands (each of the ligands is bound equatorially as well as axially). Additionally, cytotoxicity in human cancer cell lines as well as in vivo anticancer activity and general toxicity were investigated. In order to gain a deeper insight into the mode of action, pharmacologically relevant physicochemical properties of the new compounds were evaluated.

RESULTS AND DISCUSSION

Synthesis

A general reaction scheme for the preparation of novel bis- and tris-chelate diam(m)inebis(dicarboxylato)-platinum(IV) complexes is given in Figure 1. The method for synthesis was developed on the basis of the ability of diaminetetrahydroxidoplatinum(IV) complexes to undergo nucleophilic substitution reactions under acidic conditions (e.g., in carboxylic acids, which were used as reagent and solvent).[24]

The required diam(m)inetetrahydroxidoplatinum(IV) precursors were prepared by adapting a procedure reported for the synthesis of $Pt(cha)(NH_3)(OH)_4$.[25] The precursors were obtained as white to pale yellow powders with yields over 80%. Although, in some cases, elemental analysis indicated the presence of water and/or hydrogen peroxide in the samples, further purification was not necessary, as this did not disturb the next synthetic step. The target diam(m)inebis-(dicarboxylato)platinum(IV) complexes were obtained after reaction of the respective diam(m)inetetrahydroxido products with concentrated aqueous solutions of the corresponding dicarboxylic acids, forming inert five- or six-membered chelate rings. In the case of oxalic acid, diamineoxalatoplatinum(II) byproducts were also formed, most likely due to a partial reduction of the formed platinum(IV) complexes by oxalic acid. All novel compounds were obtained as white to almost white crystalline powders in yields between 25 and 70%, depending mainly on their water solubility and the method of their isolation and purification. Because protonation of Pt–OH groups is required prior to the substitution reaction with the dicarboxylate, the pH of the aqueous solution of the dicarboxylic acid and its molar concentration had a higher influence on the reaction yield than the equivalents of acid used. Moreover, the rate and yield of formation of (OC-6-22)-ethane-1,2-diaminebis(malonato)platinum(IV) (**1b**) could be increased by addition of small amounts of 0.1 M HNO_3. In contrast, the use of disodium malonate instead of malonic acid leads to decomposition of the tetrahydroxido precursor without product formation.

Characterization

The novel complexes were fully characterized by means of elemental analysis, 1D and 2D multinuclear NMR spectroscopy (^{1}H, ^{13}C, ^{15}N, and ^{195}Pt), ESI-MS, ATR-IR spectroscopy, RP-HPLC and TGA, and, in the case of **1c** and **4a**, X-ray diffraction.

All signals in the ^{1}H and ^{13}C NMR spectra were found with expected chemical shifts, and their assignment was performed on the basis of 2D $^{1}H^{1}H$ COSY, $^{1}H^{13}C$ HSQC, and $^{1}H^{13}C$ HMBC spectra. Because of the unsymmetrical character of the molecules, additional splitting of the signals could be observed. For instance, the H-2 atom resonances (see Figure

2 for NMR numbering scheme) of bis(malonato) complexes (**1–3b**) appeared as two doublets. In ^{13}C NMR spectra, two signals for C-1 and C-1′ were detected, as expected for axially or equatorially coordinated carboxylates. Analogously, splitting of the NH signals in two broad singlets could be observed for compounds **1a–d** and **2b**. In the case of diamminebis-(malonato) complex **3b**, a multiplet with coupling of ^{14}N ($^{1}J_{N,H}$ = 51.0 Hz) and ^{195}Pt ($^{2}J_{Pt,H}$ = 50.6 Hz) with the protons of the coordinated ammine ligand is visible. This is in accordance with our recent study on diamminetetracarboxylato-platinum(IV) complexes.[26] Because of the two different carrier ligands (ammonia and cyclohexylamine) in complex **5b**, additional signals in the ^{1}H and ^{13}C NMR spectra were observed. For example, the proton resonance for H-2 appeared as four doublets, whereas two differently shaped peaks were observed for the NH signals (Figure 3). Double sets of signals detected in the ^{1}H, ^{13}C, and ^{195}Pt NMR spectra of compounds **4a** and **4b** can be explained by the formation of diasteroisomers due to the chirality of the (1*R*,2*R*)-diaminocyclohexane ligand.

^{195}Pt atom resonances of complexes featuring two six-membered chelate (PtOCCCO) rings were found in the region between 3162 and 3375 ppm, in agreement with a $Pt^{IV}N_2O_4$ coordination sphere.[26-28] In the case of bis(oxalato) analogues (**1a** and **4a**), the signals were shifted upfield and observed at 2782–2815 ppm (Table S1).

Structures of the novel complexes have also been confirmed by ESI-MS spectra, measured both in the positive and negative ion mode. The most intense signals could be observed for peaks assigned to $[M - H^+]^-$ and $[M + Na^+]^+$ as well as for $[2M - H^+]^-$ and $[2M + Na^+]^+$. In some cases, signals corresponding to $[2M + Cl^-]^-$, $[M + Cl^-]^-$, and $[2M + H^+]^+$ were also detected. The *m*/*z* values and the isotopic distribution were in accordance with calculated data.

According to the elemental analysis (C, H, N, and O) and IR spectra, most of the novel compounds were isolated as hydrates. This was further proved by means of thermogravimetric analysis. The hydrated samples lost their crystal water when heated to 130 °C at a rate of 5 °C/min and flushed with air (see Figure S1 for TG/DTA curves of compound **1b**).

Most of the novel complexes demonstrated good aqueous solubility (over 20 mM for the most water-soluble agent, and between 2 and 10 mM for that with moderate solubility). However, compound **1a** seemed to be practically insoluble in water and to have very limited solubility in most organic solvents (including DMSO). Therefore, no further analytical and biological experiments were performed with this complex.

Crystal Structures

The molecular structures of complexes **1c** and **4a**, determined by single-crystal X-ray structure analysis, are shown in Figures 4 and 5, respectively, with selected bond lengths and angles quoted in the figure captions. Crystal data, data collection parameters, and structure refinement details are given in Table S2. Compound **1c** crystallized as a racemic mixture in the monoclinic space group $P2_1/n$, with molecules of cocrystallized DMF, acetone, and water. Complex **4a** crystallized as one of its diastereomeric forms in the orthorhombic space group $P2_12_12_1$, with two molecules of cocrystallized DMF. In both compounds, the Pt(IV)

atom has an octahedral coordination geometry, with one bidentate diamine ligand in the equatorial plane and two bidentate dicarboxylato ligands chelating the metal in an equatorial/axial manner. The average Pt–N and Pt–O bond lengths are 2.027(4) and 2.007(17) Å, respectively, in agreement with related octahedral Pt(IV) complexes.[9] The N–Pt–N and O–Pt–O angles in the five-membered rings formed upon ligand coordination are close to 85°, whereas in the six-membered rings (compound **1c**), the O–Pt–O angles are slightly larger than 90° (see the captions of Figures 4 and 5).

Stability in Aqueous Media under Physiologically Relevant Conditions

All novel compounds were stable within 1 h in aqueous solution as well as in phosphate-buffered saline (PBS) at pH 7.4 and 6.0 and in 0.05 M HCl. After 24 h of incubation, decomposition (<10%) was detected for compounds bearing monodentate amines (**2b** and **5b**) in PBS solution (the effect was more pronounced at pH 7.4), whereas no decomposition products were observed for complexes featuring bidentate amines (**1b–d** and **4b**). A higher level of degradation was observed only in the case of the bis(oxalato) complex (**4a**), whereas less than 45% of the native compound could be found after 24 h of incubation in PBS at pH 7.4. However, **4a** was stable in HCl solution and showed lower decomposition levels in PBS, pH 6.0 (38%), and in water (10%). Its lower stability in aqueous media (especially at physiological pH) can partially be explained with the lower thermodynamic stability of the five-membered PtOCCO ring compared to that of the respective six-membered PtOCCCO ring.

Lipophilicity

Lipophilicity is one of the most important physicochemical properties related to the pharmacokinetic behavior of drug-like molecules and their ability to cross cell membranes. The partition coefficient between water and *n*-octanol (log P) as well as the RP-HPLC-derived retention indexes (log k_w and log k_{30}) are the most commonly determined parameters, providing relevant information about the lipophilic properties of metal-based drugs.[22,26,29-33] In previous studies, we have demonstrated that cytotoxicity of diam(m)inebis- and tetrakis(carboxylato) Pt(IV) complexes increases with increasing log P, and log k_w values, respectively, within a series of closely related analogues. Remarkably, this effect is much more pronounced in the case of diam(m)inebis-(carboxylato)dichloridoplatinum(IV) complexes compared to that of their diamminetetrakis(carboxylato) analogues.[26,30,34]

Herein, we have determined the lipophilicity of novel bis- and tris-chelate compounds by measuring their retention factors (log k_w and log k_{30}) using RP-HPLC and water/MeOH mobile phases. The results are summarized in Table 1.

With the exception of **1d** and **5b**, most of the novel Pt(IV) complexes had comparable or lower log *k* values compared to the clinically used Pt(II) drugs carboplatin and oxaliplatin (cisplatin is too hydrophilic to be determined under the conditions used, as it elutes before the standard even at a 95% aqueous mobile phase). Complexes **1d** and **5b** exhibited a similar but lower lipophilicity than satraplatin, the first orally active platinum-based cytostatic.

In Vitro Cytotoxicity

Eight bis- and tris-chelate diam(m)-inebis(dicarboxylato)platinum(IV) complexes were examined with respect to their cytotoxic activity in vitro. For this purpose, a colorimetric microculture assay (MTT assay) was used in three human cancer cell lines (A549, CH1, and SW480), yielding IC_{50} values mostly in the micromolar range (Table 2). The cell line CH1 was the most sensitive, whereas the SW480 and A549 cell lines were more resistant. Overall, the range of in vitro cytotoxicity determined for the novel compounds is comparable with that previously reported for am(m)-inetetracarboxylatoplatinum(IV) complexes, prodrugs of carboplatin and oxaliplatin.[26-28] The DACH-containing complexes (**4a** and **4b**) were the most potent species in all tested cell lines, exhibiting cytotoxicity comparable or superior (in SW480 cells) to that of carboplatin. However, their antiproliferative activity is lower than that of oxaliplatin, featuring the same carrier ligand (DACH). The lower IC_{50} values observed for **4a** could be explained by its lower stability under physiologically relevant conditions, resulting in faster formation of reactive species, compared to that of **4b**. Increasing the lipophilicity via using different carboxylato ligands had a minor influence on the cytotoxicity within the series, as can be seen when comparing compounds **1b–d** (Tables 1 and 2). The activity of the novel complexes was mainly dependent on their carrier ligands and decreased as follows: DACH > NH_3/cha > $2NH_3$ > en > $2EtNH_2$. Among the bis(malonato) complexes (b series), **4b** was the most active complex. It was 6 times more active than **5b** and at least 8 times more active than **1b**, **2b**, and **3b** in SW480 cells. In A549 cells, **4b** was the only compound of the b series for which an IC_{50} value could be obtained with the chosen experimental settings. In CH1 cells, **4b** showed the same activity as **5b** but was twice as potent as **3b**, 4 times more potent than **1b**, and 12 times more potent than **2b**.

Because the carrier ligands are dictating the cytotoxic potential of the new compounds, it is of interest to determine whether this is limited only to the formation of different DNA adducts or whether alterations of other main pharmacological properties are also involved. With respect to this issue, we have performed additional studies addressing the redox behavior of the novel complexes as a function of the nature of their ligands, predominately the am(m)ines.

Redox Behavior

It is widely accepted that Pt(IV) complexes act as prodrugs, which have to be activated in vitro/in vivo to their respective active Pt(II) species. Therefore, the ease and speed of formation as well as the nature of the products to which Pt(IV) compounds will be reduced in the body are the main factors that determine their anticancer activity and systemic toxicity.[5,15] It was recently demonstrated that the rate of reduction of Pt(IV) complexes by biologically relevant reducing agents (e.g., ascorbate) depends on their axial as well as their equatorial ligands. Moreover, good correlation between electrochemically determined redox potentials and rate of reduction is valid only for complexes featuring chlorido ligands in equatorial positions.[15,26,36,37]

Since the novel bis- and tris-chelate complexes possess the same type of six-membered PtOCCCO (five-membered PtOCCO in the case of **4a**) rings as equatorial/axial leaving

groups, it was of interest to evaluate the dependence of their redox behavior on the type of the carrier ligand.

Consequently, in order to judge the influence of the carrier ligands on the time dependency of reduction of the new diam(m)inebis(dicarboxylato)platinum(IV) complexes, compounds **1b** (featuring a bidentate amine) and **5b** (featuring two different monodentate amines) were incubated with a 15-fold excess of sodium ascorbate or glutathione. Due to the H/D exchange of the acidic malonato protons, which occurs in D_2O as well as in buffered solution (pH 7.4 D_2O/H_2O), the complexes were prepared with ^{13}C=O labeled malonato ligands (**1b*** and **5b***), and $^{1}H^{13}C$ HMBC NMR spectroscopy in H_2O/D_2O (9:1) unbuffered solvent mixture was employed for monitoring of the reduction.

Compounds **1b*** and **5b*** showed similar rates of reduction in the presence of ascorbate, with a half-life of 3.4 days for **1b*** and 4.5 days for **5b***, respectively. Interestingly, reduction of **5b*** began faster, but at around 60% remaining native complex, it slowed, and at the sixth day, when **1b*** was completely reduced, 40% of **5b*** was still intact (Figure 6; Figure S2 showing comparative NMR spectra). Expectedly, the products of the reduction in both cases were the respective malonato-platinum(II) species and malonic acid. The novel bis-(dicarboxylato) complexes were reduced faster by ascorbate in comparison to their tetrakis(carboxylato) analogues ($t_{1/2}$ > 2 weeks), but were reduced much slower than bis(carboxylato)-dichloridoplatinum(IV) complexes ($t_{1/2}$ < 6 h).[26]

Glutathione was not capable of reducing the investigated compounds within 1 week of incubation. It should be mentioned that the experimental conditions used cannot represent the complicated cell microenvironment, including other reductants or mixtures thereof.

As revealed from the NMR experiments, the nature of the carrier ligands does not significantly affect the redox behavior of the new complexes. In order to estimate the influence of the size of the chelating dicarboxylate rings, we have investigated the reduction of compounds **4a** and **4b** by ascorbate with RP-HPLC. For this purpose, the complexes were incubated with a 15-fold excess of sodium ascorbate (consistent with the NMR experiments) in water and in PBS buffer (pH 7.4) at 37 °C, and their reduction was followed over 24 h. Complex **4a** could no longer be detected in PBS solution after 20 h, whereas more than 90% of **4b** was still in its native form. The rate of reduction in unbuffered solution was slower, where ~80% of **4a** and ~95% of **4b** were intact after 24 h of incubation. The results obtained for **4b** are analogous to the NMR experiments performed with bis(malonato) complexes (**1b*** and **5b***). The notably faster reduction and hydrolysis of **4a** compared to that of **4b** could explain its higher cytotoxicity in the cell lines tested and is most probably explainable by the lower thermodynamic stability of the five-membered oxalatoplatinum ring in comparison with the corresponding six-membered malonato-platinum moiety.

The HPLC experiments confirmed the formation of the respective Pt(II) species (oxaliplatin, its malonato analogue) upon reduction. A scheme of the proposed reduction pathway, proceeding via monodentate bis(malonato) (respectively, bis(oxalato)) intermediates ending up in platinum(II) species with one chelating dicarboxylato ligand, is shown in Figure S3.

Europe PMC Funders Author Manuscripts

However, platinum(II) complexes featuring two monodentate dicarboxylato ligands were not detected in our NMR and HPLC experiments as well as in ESI-MS measurements.

Theoretical Studies

The main physicochemical parameters of the new compounds related to biologically relevant properties were evaluated using DFT calculations in order to better understand their pharmacological behavior (Table 3). In the case of compounds **4a** and **4b**, calculations were performed for both diastereoisomers.

All novel complexes were calculated as being quite polar, with dipole moments varying from 10 to 18 D (Table 3). Their calculated polarizabilities increase with molecular weight, whereas a strong correlation between these two parameters was observed. The least water-soluble complexes (**1a** and **3b**) have the smallest molar volume, polarizability, and solvent-accessible surface area.

The distribution of electron density, based on the electrostatic potential (ESP), showed that the most electropositive regions in the molecules could be found around the nitrogen donor atoms and the most negative regions, around the oxygen atoms (Figure 7).

The natural population analysis (NPA) charge at Pt did not show dependence on the deviation of am(m)ine or dicarboxylato ligands; its values (1.32–1.33 au) are in good agreement with those calculated for diam(m)inetetrakis-(carboxylato)platinum(IV) complexes (prodrugs for carboplatin and oxaliplatin).[9] The low (negative) values of E_{HOMO} (<−9 eV) are a logical consequence of the inability of Pt(IV) complexes to act as reductants. Graphical representation of the frontier orbitals of complex **3b** is shown in Figure 8. The similar values observed for the adiabatic redox potential in water (around 4 eV) imply that the investigated compounds can be reduced with relatively equal effort. However, the bis(oxalato) derivatives **1a** and **4a** have slightly higher E_{red} (≥4.1 eV), which could be related to the lower stability of the five-membered PtOCCO rings.

Anticancer Activity of Complex 4b in Vivo

Compound **4b** was chosen for further investigations based on its in vitro cytotoxicity and its advantages in terms of solubility, stability, and lipophilicity. Despite complex **4a** being the most potent compound in the series, its slightly less cytotoxic bismalonato analogue (**4b**) was preferred for animal experiments due to its higher stability under physiologically relevant conditions combined with its high aqueous solubility (>15 mM). In addition, isolation and purification of **4b** is straightforward and does not require RP-HPLC (as in the case of **4a**), which is also advantageous for further comprehensive studies.

To this end, its in vivo anticancer activity was examined in a murine leukemia model (L1210, Figure 9A) and a murine colon cancer model (CT-26, Figure 9B). In all experiments, **4b** was well-tolerated with no signs of toxicity such as fatigue, weight loss, etc. With regard to its antileukemic activity, treatment with 10 mg/kg had no effect on the survival of the animals. In contrast, 20 mg/kg slightly increased the mean life span from 11.4 ± 1.2 days to 16.3 ± 3.3 days. In the group treated with 30 mg/kg, profound activity was observed, resulting in 3/4 mice being cured. With regard to the solid CT-26 model, no

significant anticancer activity was observed during the first treatment cycles. However, on day 15, complex **4b** caused distinct tumor shrinkage, resulting in significantly reduced tumor burden from 0.27 ± 0.12 g to 0.12 ± 0.04 g ($p < 0.05$). In addition, a group of mice was treated with oxaliplatin, as this is the standard therapeutic strategy against colon cancer. For these experiments, the maximal tolerated dose was applied intravenously, according to the daily oncological routine used in the clinic. These experiments revealed that in contrast to the abrupt induction of tumor shrinkage under **4b** treatment, oxaliplatin distinctly slowed tumor growth beginning from day 11 of the experiment, resulting in a final tumor volume of 0.18 ± 0.13 g. This indicates that platinum(IV) drugs might differ in their pharmacological properties from those of classic platinum(II) drugs.

To gain more insight into this issue, the total platinum content in the tumor as well as in blood, urine, and other organs (lung, liver, kidney, sciatic nerve) was subsequently determined by means of ICP-MS. The serum platinum levels 24 h after the last application of **4b** (~3 μg/mL) indicated a 10 times higher platinum circulation in the organism compared to that in the oxaliplatin-treated mice (~0.3 μg/mL). Moreover, the platinum accumulation of **4b** in tumor tissue (~5 μg/g) seemed to be superior compared to that of oxaliplatin (~1 μg/g). These findings are remarkable because the amount of platinum administered with **4b** was only 2.5 times higher in comparison to that of oxaliplatin, which indicates that **4b** might have a longer plasma half-life. The solid tissues obtained from **4b**-treated mice are ranked according to their platinum concentrations as follows (Figure S4): liver (~15 μg/g) > kidney (~10.5 μg/g) > tumor (~5 μg/g) = lung (~5 μg/g) > sciatic nerve (~1.8 μg/g). Thus, the highest amounts of platinum could be found in liver and kidney as a logical consequence of the high blood perfusion levels as well as the main role of these organs in metabolism and excretion. Notably, the pattern of platinum distribution in mice treated with **4b** differed significantly from that observed for oxaliplatin-treated mice (Figure 10). In the case of oxaliplatin, the highest platinum levels were detected in the kidney (~4.5 μg/g), whereas in the liver only ~2 μg/g was found. This is in accordance with a study on pharmacokinetics of oxaliplatin in Sprague–Dawley rats after intraperitoneal application,[38] which indicates that the platinum tissue distribution is similar after intravenous and intraperitoneal administration of oxaliplatin. Nevertheless, it has to be considered that the difference in the route of application (intraperitoneal vs intravenous) as well as the drug dose (30 vs 9 mg/kg) and molecular weight (531.37 vs 397.28 g/mol) of **4b** and oxaliplatin might impact both drug distribution as well as efficiency of excretion and thus might influence the results obtained in the study presented here. However, as there are several reports that oxaliplatin displays a similar pharmacological profile after intraperitoneal and intravenous applications,[39] the actual data might still be worth considering for further projects. Thus, our data indicate that despite the fact that both **4b** and oxaliplatin are DACH-containing complexes, their in vivo behavior turned out to differ distinctly in terms of organ distribution profile as well as kinetics of tumor response. Determining whether the difference in activity is due to the required in vivo activation of **4b** (prodrug concept) and whether the extent to which the later induced rapid tumor shrinkage is based on pronounced DNA damage and apoptosis induction are a matter of ongoing investigations.

CONCLUSIONS

Nine novel bis- and tris-chelate diam(m)inebis(dicarboxylato)-platinum(IV) complexes were synthesized and characterized in detail using various analytical techniques. Their in vitro cytotoxicity was mainly dependent on the amine carrier ligands, whereas the DACH-containing compounds proved to be the most potent species in all cell lines (CH1, SW480, and A549) tested, featuring IC_{50} values comparable or superior to that of the clinically applied drug carboplatin. On the other hand, increasing the lipophilicity via using different carboxylato ligands had only a minor effect on the cytotoxicity within the series. The pronounced anticancer and especially antileukemic activity combined with a low systemic toxicity observed in animal experiments indicates that compound **4b** might be a promising candidate for further preclinical development.

EXPERIMENTAL SECTION

All reagents and solvents were obtained from commercial suppliers and were used without further purification. Water, used in the synthetic procedures, was purified through reverse osmosis followed by double distillation. For HPLC and ICP-MS experiments, high-purity water obtained from a Milli-Q water system (18.2 MΩ cm, Milli-Q Advantage, Darmstadt, Germany) was used. ^{1}H, ^{13}C, ^{15}N, ^{195}Pt and 2D $^{1}H^{1}H$ COSY, $^{1}H^{13}C$, and $^{1}H^{15}N$ HSQC, and $^{1}H^{13}C$ HMBC NMR spectra were recorded with a Bruker Avance III 500 MHz NMR spectrometer at 500.32 (^{1}H), 125.81 (^{13}C), 107.55 (^{195}Pt), and 50.70 MHz (^{15}N) in DMF-d_7, DMSO-d_6, D_2O, or D_2O/H_2O (1:9) at ambient temperature. The splitting of proton resonances in the ^{1}H NMR spectra are defined as s = singlet, bs = broad singlet, d = doublet, dd = doublet of doublets, t = triplet, dt = doublet of triplets, and m = multiplet. ^{15}N chemical shifts were referenced relative to external NH_4Cl, whereas ^{195}Pt chemical shifts were referenced relative to external $K_2[PtCl_4]$ (see Figure 2 for the NMR numbering scheme). IR spectra were recorded with a Bruker Vertex 70 FT-IR spectrometer (4000–400 cm^{-1}) using an ATR unit. Intensities of reported IR bands are defined as br = broad, s = strong, m = medium, and w = weak. Electrospray ionization mass spectrometry was carried out with a Bruker Esquire 3000 instrument using a $MeOH/H_2O$ mixture as solvent. Elemental analyses were performed using a PerkinElmer 2400 CHN elemental analyzer and EA 3000 (for the oxygen determination) at the Microanalytical Laboratory of the University of Vienna and are within ±0.4% of the calculated values, confirming their ≥95% purity (see Table S3). Preparative RP HPLC was performed with an Agilent 1200 series system controlled by Chemstation software using an XBridge BEH C18 OBD Prep Column (19 mm × 250 mm, 5 μm). Thermogravimetric analysis (TGA) and differential thermal analysis (DTA) were carried out on a Mettler Toledo TGA/SDTA 851e instrument.

Synthesis. General Procedure for the Synthesis of Diam-(m)inetetrahydroxidoplatinum(IV) Complexes (1–5)

Pt(diam-(m)ine)I_2 (synthesized, starting from K_2PtCl_4) was converted to [Pt(diam(m)ine)$(H_2O)_2]^{2+}$ by reaction with 1.9 equiv of $AgNO_3$ in aqueous media. After filtration of the formed silver iodide, the clear solution was passed through a column, which was filled with a basic anion exchanger in order to transform the diaqua complex to its dihydroxido

analogue. Finally, Pt(diam(m)ine)$(OH)_2$ (obtained in situ) was oxidized using a 15% aqueous solution of H_2O_2. Compounds Pt(en)$(OH)_4$ (**1**), Pt$(NH_3)_2(OH)_4$ (**3**), Pt(DACH)$(OH)_4$ (**4**), and Pt(cha)$(NH_3)(OH)_4$ (**5**) have previously been described in the literature;[25,40-42] synthesis and characterization of Pt$(EtNH_2)_2(OH)_4$ (**2**) is reported for the first time herein.

(OC-6-22)-Bis(ethylamine)tetrahydroxidoplatinum(IV) (2)

$Pt(EtNH_2)_2I_2$ (1.210 g, 2.245 mmol) was suspended in water (20 mL), and $AgNO_3$ (725 mg, 4.268 mmol) was added. The reaction mixture was left stirring at RT for 20 h (light protection), whereupon the silver iodide formed was filtrated through a sintered glass funnel over a filter paper disk (MN GF-3). The clear solution obtained was passed through a column, which was filled with a basic anion exchanger (Amberlite·HCl, preconditioned with NaOH to its respective OH form[43]), all basic fractions were collected and combined, and the volume was reduced to 10 mL under reduced pressure; subsequently, the same volume of 30% H_2O_2 was added, and the reaction mixture was stirred for 15 h at RT. The volume of the dark yellow solution was then reduced under reduced pressure to ca. 2–3 mL. After cooling to 4 °C, a sufficient amount of cold acetone was added and precipitation of the product was finalized with the help of ultrasonic waves. The white precipitate formed was filtered off, washed with cold acetone, and dried in vacuo. Yield: 700 mg (88%), white to pale yellow powder. ^{1}H NMR (D_2O): δ 2.71 (m, 4H, H-3), 1.23 (t, $^3J_{H,H}$ = 7.3 Hz, 6H, H-4) ppm. ^{13}C NMR (D_2O): δ 38.8 (C-3, $^2J_{C,Pt}$ = 12.6 Hz), 14.4 (C-4, $^3J_{C,Pt}$ = 30.6 Hz) ppm. ^{195}Pt NMR (D_2O): δ 3354 ppm. IR (ATR): 3497 br (ν_{PtO-H}); 3346 br, 3097 br, 2972 br (ν_{N-H}); 1373 w, 1099 w, 1045 w cm^{-1}.

General Procedure for the Synthesis of Diam(m)inebis-(dicarboxylato)platinum(IV) Complexes

The respective diam-(m)inetetrahydroxidoplatinum(IV) complex was added to a concentrated aqueous solution of the corresponding dicarboxylic acid (8 equiv). The reaction mixture was then stirred in the dark for 1–24 h at 40–45 °C. The final products were isolated directly by filtration or via employing a combination of organic solvents for precipitation in the case of highly water-soluble compounds.

(OC-6-22)-Ethane-1,2-diaminebis(oxalato)platinum(IV) (1a)

1 (80 mg, 0.248 mmol) and oxalic acid (250 mg, 1.982 mmol) in H_2O (2 mL) were stirred for 1 h at 40 °C followed by 4 h at RT. Subsequently, the formed precipitate was filtered off, washed with water and acetone, and dried in a vacuum desiccator over P_2O_5. Yield: 56 mg (52%), almost white to pale yellow powder. ^{1}H NMR (DMSO-d_6): δ 8.35 (bs, 2H, NH_2), 8.15 (bs, 2H, NH_2), 2.64 (m, 2H, CH_2–NH_2), 2.60 (m, 2H, CH_2–NH_2) ppm. ^{13}C NMR (DMSO-d_6): δ 163.7 (C-1 or C-1′), 162.6 (C-1 or C-1′), 48.1 (C-NH_2) ppm. ^{15}N NMR (DMSO-d_6): δ −13.7 ppm. ^{195}Pt NMR (DMSO-d_6): δ 2782 ppm. IR (ATR): 3149 br, 3058 br (ν_{N-H}); 1750 m, 1714 s, 1686 m ($\nu_{C=O}$); 1354 m, 1321 w, 1043 w, 891 m cm^{-1}.

(OC-6-22)-Ethane-1,2-diaminebis(malonato)platinum(IV) (1b)

1 (100 mg, 0.294 mmol) and malonic acid (245 mg, 2.351 mmol) in H_2O (1.8 mL) were stirred for 24 h at 45 °C. The formed suspension was cooled to 4 °C, and the precipitate was filtered off and washed with a minimal amount of cold water, cold methanol, and cold acetone and dried in vacuo. Yield: 86 mg (61%), white to almost white powder. ESI MS: (positive): *m*/*z* 940.7 $[2M + Na^+]^+$, 481.7 $[M + Na^+]^+$. ESI MS (negative): *m*/*z* 915.8 $[2M - H^+]^-$, 457.6 $[M - H^+]^-$. ^{1}H NMR (DMF-d_7): δ 8.29 (bs, 2H, NH_2), 8.11 (bs, 2H, NH_2), 4.03 (d, $^2J_{H,H}$ = 15.7 Hz, 2H, H-2), 3.15 (d, $^2J_{H,H}$ = 15.7 Hz, 2H, H-2), 3.02 (m, 2H, CH_2–NH_2), 2.90 (m, 2H, CH_2–NH_2) ppm. ^{13}C NMR (DMF-d_7): δ 171.7 (C-1 or C-1′, $^2J_{Pt,C}$ = 8.1 Hz), 171.5 (C-1 or C-1′), 47.9 (C-NH_2), 46.8 (C-2) ppm. ^{15}N NMR (DMF-d_7): δ −10.1 ppm. ^{195}Pt NMR (DMF-d_7): δ 3162 ppm. IR (ATR): 3407 br (ν_{HOH}); 3273 br, 3046 br ($\nu_{N–H}$); 1701 m, 1654 s, 1629 s ($\nu_{C=O}$); 1556 m, 1354 s, 1320 m, 1206 w, 1148 w, 1044 w cm^{-1}.

(OC-6-22)-Ethane-1,2-diaminebis(3-methylmalonato)-platinum(IV) (1c)

1 (204 mg, 0.600 mmol) and 3-methylmalonic acid (555 mg, 4.700 mmol) in H_2O (2.5 mL) were stirred for 24 h at 45 °C. The clear solution formed was reduced to dryness; the residue was dissolved in a minimal amount of MeOH, and a sufficient amount of acetone was added in order to precipitate the complex. The substance was collected via filtration, washed with cold acetone, and dried in vacuo. The final pure product was obtained through recrystallization from ice-cold water. Yield: 100 mg (35%), white powder. ESI MS (positive): *m*/*z* 510.2 $[M + Na^+]^+$. ESI MS (negative): *m*/*z* 971.8 $[2M - H^+]^-$, 486.0 $[M - H^+]^-$. ^{1}H NMR (DMF-d_7): δ 8.23 (bs, 2H, NH_2), 8.03 (bs, 2H, NH_2), 4.00 (m, 2H, H-2), 3.03 (m, 2H, CH_2–NH_2), 2.90 (m, 2H, CH_2–NH_2), 1.12 (d, $^3J_{H,H}$ = 6.9 Hz, 6H, H-3) ppm. ^{13}C NMR (DMF-d_7): δ 173.3 (C-1 or C-1′, $^2J_{Pt,C}$ = 7.1 Hz), 173.1 (C-1 or C-1′), 47.8 (C-NH_2), 47.2 (C-2), 13.2 (C-3) ppm. ^{15}N (DMF-d_7) NMR: δ −9.1 ppm. ^{195}Pt NMR (DMF-d_7): δ 3171 ppm. IR (ATR): 3500 br (ν_{HOH}); 3190 br, 3148, 3067 br ($\nu_{N–H}$); 2988 br, 2948 w; 1653 s ($\nu_{C=O}$); 1569 w, 1378 m, 1364 m, 1250 m, 1208 w, 1036 w, 876 w cm^{-1}. Crystals, suitable for X-ray data collection, were obtained after vapor diffusion of a diethyl ether/acetone mixture into a DMF solution of **1c**.

(OC-6-22)-Bis(1,1-cyclobutanedicarboxylato)ethane-1,2-diamineplatinum(IV) (1d)

1 (200 mg, 0.588 mmol) and 1,1-cyclobutandicarboxylic acid (650 mg, 4.513 mmol) in H_2O (3 mL) were stirred for 20 h at 45 °C. The suspension formed was cooled to 4 °C, and the precipitate was filtered off, washed with a minimal amount of cold water and cold acetone, and dried in vacuo. Yield: 85 mg (25%), white powder. ESI MS (negative): *m*/*z* 1075.5 $[2M - H^+]^-$, 537.3 $[M - H^+]^-$. ^{1}H NMR (DMF-d_7): δ 8.07 (bs, 2H, NH_2), 7.84 (bs, 2H, NH_2), 3.00 (m, 2H, CH_2–NH_2), 2.86 (m, 2H, CH_2–NH_2), 2.73 (m, 2H, H-3 or H-3′), 2.64 (m, 4H, H-3 or H-3′), 2.39 (m, 2H, H-3 or H-3′), 1.87 (m, 4H, H-4) ppm. ^{13}C NMR (DMF-d_7): δ 176.0 (C-1 or C-1′), 175.3 (C-1 or C-1′), 55.9 (C-2), 47.7 (C-NH_2), 35.4 (C-3 or C-3′), 27.5 (C-3 or C-3′), 15.8 (C-4) ppm. ^{15}N NMR (DMF-d_7): δ −10.3 ppm. ^{195}Pt NMR (DMF-d_7):δ 3198 ppm. IR (ATR):3511 br (ν_{HOH}); 3371 br, 3052 br, 2954 br ($\nu_{N–H}$); 1622 s ($\nu_{C=O}$); 1457 w, 1336 s, 1211 w, 1096 w, 1050 w, 919 w cm^{-1}.

(OC-6-22)-Bis(ethylamine)bis(malonato)platinum(IV) (2b)

2 (200 mg, 0.566 mmol) and malonic acid (472 mg, 4.532 mmol) in H_2O (2 mL) were stirred for 22 h at 40 °C. Subsequently, the reaction mixture was reduced to dryness, and a sufficient amount of MeOH was added. The white suspension formed was cooled to 4 °C, and the product was filtered off, washed with cold acetone, and dried in vacuo. Yield: 188 mg (68%), white powder. ESI MS (positive): *m*/*z* 526.5 $[M + K^+]^+$, 510.8 $[M + Na^+]^+$. ESI MS (negative): *m*/*z* 1013.5 $[2M + Cl^-]^-$, 976.7 $[2M - H^+]^-$, 524.4 $[M + Cl^-]^-$, 488.3 $[M - H^+]^-$. ^{1}H NMR (DMF-d_7): δ 7.32 (bs, 2H, NH_2), 7.02 (bs, 2H, NH_2), 4.08 (d, $^2J_{H,H}$ = 16.0 Hz, 2H, H-2), 3.14 (d, $^2J_{H,H}$ = 15.9 Hz, 2H, H-2), 2.83 (m, 4H, H-3), 1.35 (t, $^3J_{H,H}$ = 7.3 Hz, 6H, H-4) ppm. ^{13}C NMR (DMF-d_7): δ 171.6 (C-1 or C-1′), 171.3 (C-1 or C-1′, $^2J_{Pt,C}$ = 7.2 Hz), 46.6 (C-2), 39.1 (C-3, $^2J_{Pt,C}$ = 13.9 Hz), 13.0 (C-4, $^3J_{Pt,C}$ = 31.8 Hz) ppm. ^{15}N NMR (DMF-d_7): δ −21.8 ppm. ^{195}Pt NMR (DMF-d_7): δ 3324 ppm. IR (ATR): 3127 br, 3059 br (ν_{N-H}); 2982 w; 1669 m, 1645 s, 1609 s ($\nu_{C=O}$); 1576 w, 1389 m, 1337 s, 1090 w cm^{-1}.

(OC-6-22)-Diamminebis(malonato)platinum(IV) (3b)

3 (100 mg, 0.327 mmol) and malonic acid (272 mg, 2.616 mmol) in H_2O (2 mL) were stirred for 15 h at 40 °C. Subsequently, the reaction mixture was cooled to 4 °C, and the white precipitate was filtered off, washed with a small amount of cold water and cold acetone, and dried in vacuo. Yield: 121 mg (81%), white powder. ESI MS (negative): *m*/*z* 430.8 $[M - H^+]^-$. ^{1}H NMR (DMSO-d_6): δ 6.29 (t, $^1J_{N,H}$ = 51.0 Hz, $^2J_{Pt,H}$ = 50.6 Hz, 6H, NH_3), 3.87 (d, $^2J_{H,H}$ = 16.0 Hz, 2H, H-2), 3.12 (d, $^2J_{H,H}$ = 15.9 Hz, 2H, H-2) ppm. ^{13}C NMR (DMSO-d_6): δ 172.0 (C-1 or C-1′), 171.9 (C-1 or C-1′), 47.2 (C-2) ppm. ^{15}N NMR (DMSO-d_6): δ −43.8 ppm. ^{195}Pt NMR (DMSO-d_6): δ 3375 ppm. IR (ATR): 3497 br (ν_{HOH}); 3089 br, 3046 br (ν_{N-H}); 2926 w; 1643 s, 1623 s, 1609 s ($\nu_{C=O}$); 1388 m, 1348 s, 1261 w, 1145 w, 927 w cm^{-1}.

(OC-6-22)-((1*R*,2*R*)-Diaminocyclohexane)bis(oxalato)-platinum(IV) (4a)

4 (200 mg, 0.518 mmol) and oxalic acid dihydrate (535 mg, 4.244 mmol) in H_2O (1.5 mL) were stirred for 20 min at 40 °C followed by 15 h at RT. The almost white precipitate formed was filtered off, washed with a minimal amount of water, methanol and acetone, and dried in vacuo. The presence of oxaliplatin as impurity required further purification using preparative RP-HPLC. For this purpose, MeOH/water (5:95) as the mobile phase was utilized. Afterward, the collected pure fractions were evaporated to dryness, acetone was added, and the white product was filtrated after ultrasonification and cooling to 4 °C. Yield: 60 mg (24%), white powder. ESI MS: (positive): *m*/*z* 993.0 $[2M + Na^+]^+$, 508.0 $[M + Na^+]^+$, 485.0 $[M + H^+]^+$. ESI MS (negative): *m*/*z* 968.9 $[2M - H^+]^-$, 483.2 $[M - H^+]^-$. ^{1}H NMR (DMF-d_7): δ 8.65 (bs, 2H, NH_2), 8.26 (bs, 1H, NH_2), 8.00 (bs, 1H, NH_2), 3.03 (m, 1H, H-3), 2.89 (m, 1H, H-3), 2.32 (m, 1H, H-4), 2.26 (m, 1H, H-4), 1.84 (m, 1H, H-4), 1.75 (m, 1H, H-4), 1.64 (m, 2H, H-5), 1.35 (m, 2H, H-5) ppm. ^{13}C NMR (DMF-d_7): δ 163.4 (C-1 or C-1′), 163.3 (C-1 or C-1′), 62.9 (C-3), 62.1 (C-3), 31.1 (C-4), 30.8 (C-4), 23.8 (C-5), 23.7 (C-5) ppm. ^{15}N NMR (DMF-d_7): δ −3.7 ppm. ^{195}Pt NMR (DMF-d_7): δ 2815 and 2811 ppm. IR (ATR): 3073 br, 3019 br, 2950 br (ν_{N-H}); 2867 w; 1745 m, 1710 s, 1684 s, 1657 m ($\nu_{C=O}$); 1550 w, 1543 w; 1339 s, 1293 m, 1188 w, 1065 w, 892 w, 806 m cm^{-1}. Crystals,

suitable for X-ray data collection, were obtained via vapor diffusion of an acetone/diethyl ether mixture into a DMF solution of **4a**.

(OC-6-22)-((1*R*,2*R*)-Diaminocyclohexane)bis(malonato)-platinum(IV) (4b)

4 (200 mg, 0.518 mmol) and malonic acid (451 mg, 4.334 mmol) in H_2O (1.5 mL) were stirred for 25 h at 45 °C. The suspension formed was cooled to 4 °C, and the precipitate was filtered off, washed with a minimal amount of cold water and cold acetone, and dried in vacuo. Yield: 69 mg (26%), white to almost white powder. ESI MS: (positive): *m*/*z* 1048.4 $[2M + Na^+]^+$, 535.3 $[M + Na^+]^+$. ESI MS (negative): *m*/*z* 1024.3 $[2M - H^+]^-$, 510.1 $[M - H^+]^-$. ^{1}H NMR (DMF-d_7): δ 8.47 (bs, 1H, NH_2), 8.36 (bs, 1H, NH_2), 7.93 (bs, 1H, NH_2), 7.88 (bs, 1H, NH_2), 4.03 (d, $^2J_{H,H}$ = 15.8 Hz, 1H, H-2), 4.02 (d, $^2J_{H,H}$ = 15.7 Hz, 1H, H-2), 3.18 (d, $^2J_{H,H}$ = 15.8 Hz, 1H, H-2), 3.14 (d, $^2J_{H,H}$ = 15.7 Hz, 1H, H-2), 2.98 (m, 1H, H-3), 2.91 (m, 1H, H-3), 2.27 (m, 2H, H-4), 1.84 (m, 1H, H-4), 1.75 (m, 1H, H-4), 1.62 (m, 2H, H-5), 1.31 (m, 2H, H-5) ppm. ^{13}C NMR (DMF-d_7): δ 171.8 (C-1 or C-1′), 171.7 (C-1 or C-1′), 171.5 (C-1 or C-1′), 62.0 (C-3), 61.7 (C-3), 47.0 (C-2), 46.7 (C-2), 30.7 (C-4), 30.5 (C-4), 23.8 (C-5), 23.7 (C-5) ppm. ^{15}N NMR (DMF-d_7): δ 0.9 ppm. ^{195}Pt NMR (DMF-d_7): δ 3206 and 3198 ppm. IR (ATR): 3513 br (ν_{HOH}); 3164 br, 3070 br, 3010 br, 2944 br (ν_{N-H}); 1667 m, 1640 s ($\nu_{C=O}$); 1576 w, 1377 w, 1330 m, 1289 m, 1153 w, 923 w cm^{-1}.

(OC-6-32)-Ammine(cyclohexylamine)bis(malonato)-platinum(IV) (5b)

5 (190 mg, 0.479 mmol) and malonic acid (406 mg, 3.902 mmol) in H_2O (2.5 mL) were stirred for 20 h at 40 °C. The turbid yellow solution obtained was filtrated through a sintered glass funnel (covered with a filter paper disk, MN GF-3) and evaporated to dryness. Subsequently, the product was suspended in a cold mixture of MeOH and acetone and collected via filtration. The white powder obtained was recrystallized from a minimal amount of ice-cold water, filtered off, washed with a minimal amount of cold water and cold acetone, and dried in vacuo. Yield: 105 mg (42%), white powder. ESI MS: (positive): *m*/*z* 1051.5 $[2M + Na^+]^+$, 1030.5 $[2M + H^+]^+$. ESI MS (negative): *m*/*z* 1063.4 $[2M + Cl^-]^-$, 1028.5 $[2M - H^+]^-$, 513.5 $[M - H^+]^-$. ^{1}H NMR (DMF-d_7): δ 7.21 (bs, 1H, NH_2), 6.97 (bs, 1H, NH_2), 6.61 (t, $^1J_{N,H}$ = 52.6 Hz, $^2J_{Pt,H}$ = 51.4 Hz, 3H, NH_3), 4.07 (d, $^2J_{H,H}$ = 16.0 Hz, 1H, H-2/H-2′), 4.06 ($^2J_{H,H}$ = 15.8 Hz, 1H, H-2/H-2′), 3.16 (d, $^2J_{H,H}$ = 16.0 Hz, 1H, H-2/H-2′), 3.14 (d, $^2J_{H,H}$ = 15.8 Hz, 1H, H-2/H-2′), 2.85 (m, 1H, H-3), 2.23 (m, 1H, H-4 or H-4′), 2.16 (m, 1H, H-4 or H-4′), 1.73 (m, 2H, H-5 or H-5′), 1.61 (m, 1H, H-6), 1.45 (m, 2H, H-4 or H-4′), 1.30 (m, 2H, H-5 or H-5′), 1.16 (m, 1H, H-6) ppm. ^{13}C NMR (DMF-d_7): δ 171.7 (C-1, C-1′, C-1″ or C-1‴), 171.6 (C-1, C-1′, C-1″ or C-1‴), 171.3 (C-1, C-1′, C-1″ or C-1‴), 54.2 (C-3, $^2J_{Pt,C}$ = 10.6 Hz), 46.7 (C-2 or C-2′), 46.6 (C-2 or C-2′), 32.1 (C-4 or C-4′, $^3J_{Pt,C}$ = 20.2 Hz), 31.7 (C-4 or C-4′, $^3J_{Pt,C}$ = 12.1 Hz), 25.2 (C-6), 24.9 (C-5 or C-5′), 24.7 (C-5 or C-5′) ppm. ^{15}N NMR (DMF-d_7): δ −12.2 (NH_2), −44.0 (NH_3) ppm. ^{195}Pt NMR (DMF-d_7): δ 3370 ppm. IR (ATR): 3554 br, 3477 br (ν_{HOH}); 3043 br (ν_{N-H}); 2929 br; 1630 s ($\nu_{C=O}$); 1373 m, 1331 s, 1258 w, 927 w cm^{-1}.

(OC-6-22)-Ethane-1,2-diaminebis(1,3-$^{13}C_2$-malonato)-platinum(IV) (1b*)

To a mixture of **1** (50 mg, 0.147 mmol) and 1,3-$^{13}C_2$-malonic acid (63 mg, 0.592 mmol) in water (0.7 mL) was added 0.1 M HNO_3 (80 μL), and the mixture was stirred for 24 h at 45

°C. Subsequently, the reaction mixture was cooled to 4 °C, and the precipitate formed was filtered off, washed with a small amount of cold water and cold acetone, and dried in vacuo. Yield: 35 mg (50%), white to almost white powder. ESI MS (negative): *m*/*z* 923.8 [2M − H^+]$^-$, 460.7 [M − H^+]$^-$. ^{1}H NMR (DMF-d_7): δ 8.30 (bs, 2H, NH_2), 8.12 (bs, 2H, NH), 4.03 (dt, $^2J_{H,H}$ = 15.7 Hz, $^2J_{C,H}$ = 8.9 Hz, $^2J_{C,H}$ = 6.9 Hz, 2H, H-2), 3.15 (dt, $^2J_{H,H}$ = 15.7 Hz, $^2J_{C,H}$ = 5.4 Hz, 2H, H-2), 3.02 (m, 2H, CH_2–NH_2), 2.90 (m, 2H, CH_2–NH_2) ppm. ^{13}C NMR (DMF-d_7): δ 171.7 (d, $^2J_{C,C}$ = 1.9 Hz, $^2J_{C,Pt}$ = 8.1 Hz, C-1 or C-1′), 171.6 (d, $^2J_{C,C}$ = 2.4 Hz, C-1 or C-1′), 47.9 (C-NH), 46.8 (t, $^1J_{C,C}$ = 50.2 Hz, C-2) ppm. ^{15}N NMR (DMF-d_7): δ −9.9 ppm. ^{195}Pt NMR (DMF-d_7): δ = 3160 ppm.

(OC-6-32)-Ammine(cyclohexylamine)bis(1,3-$^{13}C_2$-malonato)-platinum(IV) (5b*)

5 (80 mg, 0.202 mmol) and 1,3-$^{13}C_2$-malonic acid (92 mg, 0.868 mmol) in H_2O (1 mL) were stirred for 20 h at 40 °C. The turbid yellow solution obtained was filtered through a sintered glass funnel (covered with a filter paper disk, MN GF-3) and evaporated to dryness. Subsequently, the product was suspended in a cold mixture of MeOH and acetone, collected via filtration, washed with cold acetone, and dried in vacuo. Yield: 65 mg (61%), white powder. ESI MS: (positive): *m*/*z* 1058.7 [2M + Na^+]$^+$. ESI MS (negative): *m*/*z* 1037.0 [2M − H^+]$^-$, 517.3 [M − H^+]$^-$. ^{1}H NMR (DMF-d_7): δ 7.20 (bs, 1H, NH_2), 6.96 (bs, 1H, NH), 6.60 (t, $^1J_{N,H}$ = 52.7 Hz, $^2J_{Pt,H}$ = 51.5 Hz, 3H, NH_3), 4.06 (m, 2H, H-2), 3.15 (m, 2H, H-2), 2.85 (m, 1H, H-3), 2.23 (m, 1H, H-4 or H-4′), 2.15 (m, 1H, H-4 or H-4′), 1.74 (m, 2H, H-5 or H-5′), 1.61 (m, 1H, H-6), 1.45 (m, 2H, H-4 or H-4′), 1.30 (m, 2H, H-5 or H-5′), 1.17 (m, 1H, H-6) ppm. ^{13}C NMR (DMF-d_7): δ 171.7 (d, $^2J_{C,C}$ = 2.7 Hz, C-1, C-1′, C-1″ or C-1‴), 171.6 (d, $^2J_{C,C}$ = 2.9 Hz, C-1, C-1′, C-1″ or C-1‴), 171.4 (d, $^2J_{C,C}$ = 2.1 Hz, C-1, C-1′, C-1″ or C-1‴), 54.2 (C-3, $^2J_{Pt,Ct}$ = 10.1 Hz), 46.7 (t, $^1J_{C,C}$ = 50.1 Hz, C-2 or C-2′), 46.6 (t, $^1J_{C,C}$ = 50.2 Hz C-2 or C-2′), 32.1 (C-4 or C-4′, $^3J_{Pt,C}$ = 19.3 Hz), 31.7 (C-4 or C-4′, $^3J_{Pt,C}$ = 11.6 Hz), 25.2 (C-6), 24.9 (C-5 or C-5′), 24.7 (C-5 or C-5′) ppm. ^{15}N NMR (DMF-d_7): δ −11.6 (NH_2), −44.0 (NH_3) ppm. ^{195}Pt NMR (DMF-d_7): δ 3369 ppm.

Crystallographic Structure Determination

X-ray diffraction measurements for **1c** and **4a** were performed with a Bruker X8 APEXII and Bruker D8 Venture CCD diffractometer, respectively. Single crystals of **1c** and **4a** were positioned at 35 and 45 mm from the detector, and 607 and 913 frames were measured, each for 5 and 30 s over 1 or 0.5° scan width, respectively. The data were processed using SAINT software.[44] Crystal data, data collection parameters, and structure refinement details are given in Table S2. The structure was solved by direct methods and refined by full-matrix least-squares techniques. Non-hydrogen atoms were refined with anisotropic displacement parameters. Hydrogen atoms were inserted in calculated positions and refined with a riding model. One molecule of cocrystallized dimethylformamide (DMF) and one molecule of water were found disordered over two positions with S.O.F. 0.7 to 0.3 in **1c**, whereas in **4a**, one molecule of DMF was disordered over two positions with S.O.F. 0.6:0.4. The disorder was resolved by using SADI, DFIX, and EADP restraints/constraints implemented in SHELXL. The following computer programs were used: structure solution, SHELXS-97; structure refinement, SHELXL-97;[45] molecular graphics, Mercury 3.0.

Determination of Lipophilicity

Lipophilicity of the new compounds is expressed as the chromatographic retention factors (namely, log k_w and log k_{30}) using reversed-phased HPLC. The analysis was performed on a Dionex Summit system controlled by the Dionex Chromeleon 6.80 software. The samples were prepared by dissolving of around 0.3–0.5 mg of each complex in 1 mL of a H_2O/MeOH (7:3) mixture, followed by filtration through a 0.2 μm Nylon filter. The chromatographic conditions were as follows: Agilent ZORBAX SB aq C18 column (4.6 mm × 250 mm, 5 μm); injection volume, 20 μL; flow rate, 1 mL/min; isocratic elution; temperature of the column, 25 °C; UV–vis detection set up at 210 nm; KI was used as an internal reference to determine the column dead-time (t_0); mobile phases containing different percentage of 0.1% TFA aqueous solution and MeOH (the MeOH fraction ranged from 50% for the most lipophilic compounds to 5% for the most hydrophilic ones); chromatograms for each complex were run with at least three different mobile phase compositions and at least two times.

The capacity factors $k = (t_R - t_0)/t_0$ (t_R is the retention time of the species analyzed and t_0 is the retention time of KI) of the investigated compounds were calculated for all eluent compositions. The partition between the lipophilic stationary phase and water (0% MeOH) was determined by extrapolation using the linear Soczewinski–Snyder relationship[46,47] between log k and the concentration of the organic modifier in the mobile phase

$$\log k = \log k_w - S_\varphi$$

where log k is the capacity factor in the specific mobile phase composition, φ is the volume fraction of MeOH in the eluent, S is a constant for a given solute and a given HPLC system, and log k_w corresponds to log k in pure water (buffer).

Stability under Physiological Conditions

The novel complexes (c = 0.5 mM) were incubated in water, PBS solution (pH 7.4 and 6.0), and 0.05 M HCl (pH 1.5) at 37 °C for 24 h. Their stability after 1 and 24 h was measured by means of RP-HPLC, applying the same chromatographic conditions used for the lipophilicity determination; mobile phases consisted of an appropriate 0.1% TFA water/MeOH ratio in order to achieve elution of the compounds within 15 min.

Incubation with Ascorbate and Glutathione

Reduction of complexes **1b*** and **5b*** (^{13}C=O labeled **1b** and **5b**) by sodium ascorbate and by glutathione was monitored by $^1H^{13}C$ HMBC NMR spectroscopy at ambient temperature. Solutions of the compounds (2 mM) were prepared in D_2O/H_2O (1:9); sodium ascorbate (30 mM) or glutathione (30 mM), respectively, was added, and $^1H^{13}C$ HMBC NMR spectra were recorded for 6 days. The reduction was monitored by following the decrease of intensity of malonato $CH_2/^{13}C$=O cross peaks from the complexes at 4.12/174.8 ppm, 4.06/174.6 ppm and 3.38/175.1 ppm for **1b***, and at 4.20/174.7 ppm, 4.16/174.3 ppm, 4.09/174.9 ppm, and 3.39/175.1 ppm for **5b*** relative to the increase of signals of the

reduced species at 3.52/178.0 ppm and 3.10/176.8 ppm for **1b*** and at 3.59/178.1 ppm and 3.09/176.3 ppm for **5b***.

In addition, compounds **4a** and **4b** (0.5 mM) were incubated with a 15-fold excess of sodium ascorbate in water and PBS solution (pH 7.4) at 37 °C, and their reduction was followed by means of RP-HPLC over 24 h. The analysis was performed on a Dionex Ultimate 3000 RS system, controlled by the Dionex Chromeleon 6.80 software. The chromatographic conditions were as follows: Poroshell 120 SB C18 column (2.1 mm × 150 mm, 2.7 μm); injection volume, 2 μL; flow rate, 0.2 mL/min; temperature of the column, 25 °C; UV–vis detection set up at 210 nm; mobile phase consisted of 0.1% TFA water/MeOH (95:5).

Theoretical Calculations

All calculations were performed with the Gaussian 09 software package.[48] The starting structures for optimizations were taken from the X-ray data of complexes **1c** and **4a**. The other compounds were modeled by modification of the latter.

The DFT long-range corrected hybrid wb97x functional was used for all calculations[49] in connection with the Def2-SVP basis set[50] with effective core potential[51] for optimizing geometries and calculation of physicochemical properties of interest. Geometry optimizations were performed in the gas phase and in a water solvent model by using the IEFPCM[52] method. Solvent-accessible surface area (SASA) was extracted after single-point energy calculation of gas-phase-optimized structures in water environment with the ipcm[53] method, where the cavity is defined by a self-consistent isodensity contour in a water solvent model. Atomic charges were calculated using the NPA approach.[54]

The molar volumes, dipole moments, polarizabilities, and energies of the frontier orbitals were taken from the gas-phase-optimized geometries. The energies of hydration were calculated by extracting the energies in water environment from total energies in the gas phase. For estimation of redox potentials, geometries of the corresponding anion radicals were optimized in water, and their energies were extracted from the energies of the neutral complexes also optimized in water, employing the IEFPCM solvation model.

Cell Lines and Cell Culture Conditions

For cytotoxicity determination, three different human cancer cell lines were used: A549 (nonsmall cell lung cancer) and SW480 (colon carcinoma), both kindly provided by Brigitte Marian, Institute of Cancer Research, Department of Medicine I, Medical University Vienna, Austria, as well as CH1 (ovarian carcinoma), kindly provided by Lloyd R. Kelland, CRC Centre for Cancer Therapeutics, Institute of Cancer Research, Sutton, U.K. All cell culture media and reagents were purchased from Sigma-Aldrich Austria, unless otherwise indicated. Cells were grown as adherent monolayer cultures in 75 cm^2 culture flasks (StarLab, CytoOne) in minimal essential medium supplemented with 10% heat-inactivated fetal bovine serum (Invitrogen), 1 mM sodium pyruvate, 1% v/v nonessential amino acids (from 100× ready-to-use stock), and 4 mM L-glutamine without antibiotics at 37 °C under a humidified atmosphere containing 5% CO_2 and 95% air.

Europe PMC Funders Author Manuscripts

Cytotoxicity Assay

Cytotoxicity was determined by the colorimetric MTT assay (MTT = 3-(4,5-dimethyl-2-thiazolyl)-2,5-diphenyl-2*H*-tetrazolium bromide) as described previously.[22] Briefly, cells were harvested by trypsinization and seeded in medium (vide supra) into 96-well plates in volumes of 100 μL/well. Depending on the cell line, different cell densities were used to ensure exponential growth of the untreated controls during the experiment: 1.0×10^3 (CH1), 2.0×10^3 (SW480), and 3.0×10^3 (A549) cells per well. In the first 24 h, the cells were allowed to settle and resume exponential growth. Then, the test compounds were dissolved in medium, serially diluted in medium, and added to the plates in volumes of 100 μL/well. After continuous exposure for 96 h (in the incubator at 37 °C and under 5% CO_2), the medium was replaced with 100 μL/well RPMI 1640 medium (supplemented with 10% heat-inactivated fetal bovine serum and 4 mM L-glutamine) and MTT solution (MTT reagent in phosphate-buffered saline, 5 mg/mL) in a ratio of 6:1, and plates were incubated for a further 4 h. Then, the medium/MTT mixture was removed, and the formed formazan was dissolved in DMSO (150 μL/well). Optical densities at 550 nm were measured (reference wavelength, 690 nm) with a microplate reader (ELX880, BioTek). The quantity of viable cells was expressed as a percentage of untreated controls, and 50% inhibitory concentrations (IC_{50}) were calculated from the concentration–effect curves by interpolation. Every test was repeated in at least three independent experiments, each consisting of three replicates per concentration level.

Antileukemic Activity in Vivo

L1210 murine leukemia cells (1×10^5) were injected intraperitoneally in a volume of 0.2 mL into female DBA/2J × Balb/c SCID F1 mice on day 0. Compound **4b** (dissolved in water) was administered intraperitoneally at drug concentrations of 10, 20, and 30 mg/kg on days 1, 5, and 9. Toxicity was monitored by daily observation of animals and registration of their body weight. Therapeutic efficacy of the drug candidate was monitored by recording the length of survival of experimental mice compared to that of untreated control animals. Experiments were carried out according to the Austrian and FELASA guidelines for animal care and protection.

Anticancer Activity Against CT-26 Cells in Vivo

Six- to eight-week-old female Balb/c mice were purchased from Harlan Laboratories (San Pietro al Natisone, Italy). The animals were kept in a pathogen-free environment, and every procedure was performed in a laminar airflow cabinet. Experiments were approved by the local ethics commission and carried out according to the Austrian and FELASA guidelines for animal care and protection. Murine CT-26 cells (5×10^5) were injected subcutaneously into the right flank. Therapy was started when tumor nodules were palpable. Animals were treated with complex **4b** (dissolved in water) intraperitoneally at a drug concentration of 30 mg/kg or with oxaliplatin (dissolved in 5% glucose) intravenously at a drug concentration of 9 mg/kg (maximal tolerated dose) twice a week for 2 weeks. Animals were controlled for distress development every day, and tumor size was assessed regularly by caliper measurement. Tumor volume was calculated using the formula $(\text{length} \times \text{width}^2)/2$. The experiment had to be terminated on day 15 due to ulceration of the tumors in the control

group. Animals were anesthetized 24 h after the last treatment, and blood was collected by heart punctuation. Serum was isolated by centrifugation of the collected blood samples at 3000 rpm for 10 min for two times and stored at −20 °C. In addition, samples of organs and tumor tissue were stored at −20 °C for the quantitative determination of platinum by means of ICP-MS.

Determination of the Platinum Concentration in Mouse Tissues by ICP-MS

Digestion of mouse tissue samples (tumor, kidney, liver, lung, and nerve) as well as blood pellet and serum was performed using a microwave system Discover SP-D (CEM Microwave Technology, Germany) with sub-boiled nitric acid (≥65%, p.a., Fluka). Samples were diluted with Milli-Q water, resulting in nitric acid concentrations lower than 3% and platinum concentrations lower than 15 μg/g. The total platinum content was determined with an ICP-Triple-Quadrupole MS instrument Agilent 8800 (Agilent Technologies, Tokyo, Japan) equipped with a MicroMist nebulizer at a sample uptake rate of approximately 0.25 mL/min. Platinum and rhenium standards were derived from CPI International (Amsterdam, The Netherlands), whereas Re served as the internal standard for Pt. Quantification was done using the isotopes ^{185}Re and ^{195}Pt with a dwell time of 0.3 s and 10 replicates. The instrument was equipped with nickel cones and was operated at an RF power of 1550 W, with argon as plasma gas (15 L/min) as well as carrier gas (1.10 L/min). The MassHunter software package (Workstation Software, version B.01.03, 2013) was used for data processing.

Supplementary Material

Refer to Web version on PubMed Central for supplementary material.

ACKNOWLEDGMENTS

The authors thank Dr. P. Unfried for measuring TG/DTA. H.P.V. is thankful for financial support from the University of Vienna within the doctoral program Initiativkolleg Functional Molecules IKI041-N. The authors are indebted to the FFG, Research and Technology Development, the FWF (Austrian Science Fund, P20683-N19 and L568-B11), and COST CM1105. The authors acknowledge financial support of the Austrian Science Fund (FWF) and grant P26603 (to P.H.). We are thankful to S. van Schoonhoven and G. Zeitler for animal care.

ABBREVIATIONS USED

DFT	density functional theory
TGA	thermogravimetric analysis
en	ethane-1,2-diamine
cha	cyclohexylamine
DACH	(1*R*,2*R*)-diaminocyclohexane
CBDCA	1,1-cyclobutanedicarboxylate
PBS	phosphate buffered saline
ESP	electrostatic potential

NPA natural population analysis

REFERENCES

(1). Wheate NJ, Walker S, Craig GE, Oun R. The status of platinum anticancer drugs in the clinic and in clinical trials. Dalton Trans. 2010; 39:8113–8127. [PubMed: 20593091]

(2). Einhorn, LH. Cisplatin and the revolution of treatment of germ cell tumors; 11th International Symposium on Platinum Coordination Compounds in Cancer Chemotherapy; Verona, Italy. October 11–14, 2012;

(3). Galanski M, Jakupec MA, Keppler BK. Update of the preclinical situation of anticancer platinum complexes: novel design strategies and innovative analytical approaches. Curr. Med. Chem. 2005; 12:2075–2094. [PubMed: 16101495]

(4). Kelland L. The resurgence of platinum-based cancer chemotherapy. Nat. Rev. Cancer. 2007; 7:573–584. [PubMed: 17625587]

(5). Graf N, Lippard SJ. Redox activation of metal-based prodrugs as a strategy for drug delivery. Adv. Drug Delivery Rev. 2012; 64:993–1004.

(6). Hall MD, Mellor HR, Callaghan R, Hambley TW. Basis for design and development of platinum(IV) anticancer complexes. J. Med. Chem. 2007; 50:3403–3411. [PubMed: 17602547]

(7). Harper BW, Krause-Heuer AM, Grant MP, Manohar M, Garbutcheon-Singh KB, Aldrich-Wright JR. Advances in platinum chemotherapeutics. Chem.—Eur. J. 2010; 16:7064–7077. [PubMed: 20533453]

(8). Johnstone TC, Wilson JJ, Lippard SJ. Monofunctional and higher-valent platinum anticancer agents. Inorg. Chem. 2013; 52:12234–12249. [PubMed: 23738524]

(9). Varbanov HP, Jakupec MA, Roller A, Jensen F, Galanski M, Keppler BK. Theoretical investigations and density functional theory based quantitative structure-activity relationships model for novel cytotoxic platinum(IV) complexes. J. Med. Chem. 2013; 56:330–344. [PubMed: 23214999]

(10). Wilson JJ, Lippard SJ. Synthetic methods for the preparation of platinum anticancer complexes. Chem. Rev. 2014; 114:4470–4495. [PubMed: 24283498]

(11). Sova P, Mistr A, Kroutil A, Semerad M, Chlubnova H, Hruskova V, Chladkova J, Chladek J. A comparative study of pharmacokinetics, urinary excretion and tissue distribution of platinum in rats following a single-dose oral administration of two platinum(IV) complexes LA-12 (OC-6-43)-bis(acetato)(1-adamantylamine)-amminedichloroplatinum(IV) and satraplatin (OC-6-43)-bis(acetato)-amminedichloro(cyclohexylamine)platinum(IV). Cancer Chemother. Pharmacol. 2011; 67:1247–1256. [PubMed: 20697713]

(12). Hall MD, Hambley TW. Platinum(IV) antitumour compounds: their bioinorganic chemistry. Coord. Chem. Rev. 2002; 232:49–67.

(13). Galanski M, Keppler BK. Is reduction required for antitumour activity of platinum(IV) compounds? Characterisation of a platinum(IV)–nucleotide adduct [enPt($OCOCH_3$)$_3$(5′-GMP)] by NMR spectroscopy and ESI-MS. Inorg. Chim. Acta. 2000; 300-302:783–789.

(14). Schilder RJ, LaCreta FP, Perez RP, Johnson SW, Brennan JM, Rogatko A, Nash S, McAleer C, Hamilton TC, Roby D, et al. Phase I and pharmacokinetic study of ormaplatin (tetraplatin, NSC 363812) administered on a day 1 and day 8 schedule. Cancer Res. 1994; 54:709–717. [PubMed: 8306332]

(15). Chen CKJ, Zhang JZ, Aitken JB, Hambley TW. Influence of equatorial and axial carboxylato ligands on the kinetic inertness of platinum(IV) complexes in the presence of ascorbate and cysteine and within DLD 1 cancer cells. J. Med. Chem. 2013; 56:8757–8764. [PubMed: 24107138]

(16). Barefoot RR. Speciation of platinum compounds: a review of recent applications in studies of platinum anticancer drugs. J. Chromatogr. B. 2001; 751:205–211.

Europe PMC Funders Author Manuscripts

(17). Raynaud FI, Mistry P, Donaghue A, Poon GK, Kelland LR, Barnard CFJ, Murrer BA, Harrap KR. Biotransformation of the platinum drug JM216 following oral administration to cancer patients. Cancer Chemother. Pharmacol. 1996; 38:155–162. [PubMed: 8616906]

(18). Carr JL, Tingle MD, McKeage MJ. Satraplatin activation by haemoglobin, cytochrome C and liver microsomes in vitro. Cancer Chemother. Pharmacol. 2006; 57:483–490. [PubMed: 16172904]

(19). Margiotta N, Ranaldo R, Intini FP, Natile G. Cationic intermediates in oxidative addition reactions of Cl_2 to [$PtCl_2$(cis-1,4-DACH)]. Dalton Trans. 2011; 40:12877–12885. [PubMed: 22064914]

(20). Chin CF, Tian Q, Setyawati MI, Fang W, Tan ESQ, Leong DT, Ang WH. Tuning the activity of platinum(IV) anticancer complexes through asymmetric acylation. J. Med. Chem. 2012; 55:7571–7582. [PubMed: 22876932]

(21). Feazell RP, Nakayama-Ratchford N, Dai H, Lippard SJ. Soluble single-walled carbon nanotubes as longboat delivery systems for platinum(IV) anticancer drug design. J. Am. Chem. Soc. 2007; 129:8438–8439. [PubMed: 17569542]

(22). Pichler V, Goeschl S, Meier SM, Roller A, Jakupec MA, Galanski M, Keppler BK. Bulky N,N-(di)alkylethane-1,2-diamineplatinum(II) compounds as precursors for generating unsymmetrically substituted platinum(IV) complexes. Inorg. Chem. 2013; 52:8151–8162. [PubMed: 23790208]

(23). Zhang JZ, Bonnitcha P, Wexselblatt E, Klein AV, Najajreh Y, Gibson D, Hambley TW. Facile preparation of mono-, di- and mixed-carboxylato platinum(IV) complexes for versatile anticancer prodrug design. Chem.—Eur. J. 2013; 19:1672–1676. [PubMed: 23255183]

(24). Song R, Kim KM, Sohn YS. Synthesis and characterization of novel tricarboxylatoplatinum(IV) complexes. Nucleophilic substitution of (diamine)-tetrahydroxoplatinum(IV) with carboxylic acid. Inorg. Chim. Acta. 2002; 338:89–93.

(25). Barnard CFJ, Vollano JF, Chaloner PA, Dewa SZ. Studies on the oral anticancer drug JM-216: synthesis and characterization of isomers and related complexes. Inorg. Chem. 1996; 35:3280–3284. [PubMed: 11666529]

(26). Varbanov HP, Valiahdi SM, Kowol CR, Jakupec MA, Galanski M, Keppler BK. Novel tetracarboxylatoplatinum(IV) complexes as carboplatin prodrugs. Dalton Trans. 2012; 41:14404–14415. [PubMed: 22886297]

(27). Reithofer MR, Valiahdi SM, Jakupec MA, Arion VB, Egger A, Galanski M, Keppler BK. Novel di- and tetracarboxylatoplatinum(IV) complexes. Synthesis, characterization, cytotoxic activity, and DNA platination. J. Med. Chem. 2007; 50:6692–6699. [PubMed: 18031001]

(28). Hoffmeister BR, Adib-Razavi MS, Jakupec MA, Galanski M, Keppler BK. Diamminetetrakis(carboxylato)platinum(IV) complexes—synthesis, characterization, and cytotoxicity. Chem. Biodiversity. 2012; 9:1840–1848.

(29). Platts JA, Oldfield SP, Reif MM, Palmucci A, Gabano E, Osella D. The RP-HPLC measurement and QSPR analysis of log$P_{o/w}$ values of several Pt(II) complexes. J. Inorg. Biochem. 2006; 100:1199–1207. [PubMed: 16530269]

(30). Reithofer MR, Bytzek AK, Valiahdi SM, Kowol CR, Groessl M, Hartinger CG, Jakupec MA, Galanski M, Keppler BK. Tuning of lipophilicity and cytotoxic potency by structural variation of anticancer platinum(IV) complexes. J. Inorg. Biochem. 2011; 105:46–51. [PubMed: 21134601]

(31). Valko K. Application of high-performance liquid chromatography based measurements of lipophilicity to model biological distribution. J. Chromatogr. A. 2004; 1037:299–310. [PubMed: 15214672]

(32). Nasal A, Siluk D, Kaliszan R. Chromatographic retention parameters in medicinal chemistry and molecular pharmacology. Curr. Med. Chem. 2003; 10:381–426. [PubMed: 12570698]

(33). Ermondi G, Caron G, Ravera M, Gabano E, Bianco S, Platts JA, Osella D. Molecular interaction fields vs. quantum-mechanical-based descriptors in the modelling of lipophilicity of platinum(IV) complexes. Dalton Trans. 2013; 42:3482–3489. [PubMed: 23263457]

(34). Varbanov H, Valiahdi SM, Legin AA, Jakupec MA, Roller A, Galanski M, Keppler BK. Synthesis and characterization of novel bis(carboxylato)dichloridobis(ethylamine)platinum(IV)

complexes with higher cytotoxicity than cisplatin. Eur. J. Med. Chem. 2011; 46:5456–5464. [PubMed: 21940073]

(35). Banfić J, Legin AA, Jakupec MA, Galanski M, Keppler BK. Platinum(IV) complexes featuring one or two axial ferrocene bearing ligands — synthesis, characterization, and cytotoxicity. Eur. J. Inorg. Chem. 2014; 2014:484–492.

(36). Zhang JZ, Wexselblatt E, Hambley TW, Gibson D. Pt(IV) analogs of oxaliplatin that do not follow the expected correlation between electrochemical reduction potential and rate of reduction by ascorbate. Chem. Commun. 2012; 48:847–849.

(37). Wexselblatt E, Gibson D. What do we know about the reduction of Pt(IV) pro-drugs? J. Inorg. Biochem. 2012; 117:220–229. [PubMed: 22877926]

(38). Pestieau SR, Belliveau JF, Griffin H, Stuart OA, Sugarbaker PH. Pharmacokinetics of intraperitoneal oxaliplatin: experimental studies. J. Surg. Oncol. 2001; 76:106–114. [PubMed: 11223836]

(39). Jerremalm E, Wallin I, Ehrsson H. New insights into the biotransformation and pharmacokinetics of oxaliplatin. J. Pharm. Sci. 2009; 98:3879–3885. [PubMed: 19340883]

(40). Zheligovskaya, NN.; Melnikov, MY. Method for producing platinum(IV) complexes. WO2003066526A1. 2003.

(41). Kim KM, Lee Y-A, Lee SS, Sohn YS. Facile synthesis and structural properties of (diamine)tetracarboxylatoplatinum(IV) complexes. Inorg. Chim. Acta. 1999; 292:52–56.

(42). Brandon RJ, Dabrowiak JC. Synthesis, characterization, and properties, of a group of platinum(IV) complexes. J. Med. Chem. 1984; 27:861–865. [PubMed: 6330359]

(43). Meelich K, Galanski M, Arion VB, Keppler BK. Bis(2-amino alcohol-κN)dicarboxylatoplatinum(II) complexes—elegant synthesis via ring-opening of bis(2-amino alcoholato-κ2N,O)platinum(II) species with dicarboxylic acids. Eur. J. Inorg. Chem. 2006:2476–2483.

(44). *SAINT-Plus*, version 7.06a, and APEX2. Bruker-Nonius AXS Inc.; Madison, WI: 2004.

(45). Sheldrick GM. A short history of SHELX. Acta Crystallogr., Sect. A. 2008; 64:112–122. [PubMed: 18156677]

(46). Soczewinski E, Wachtmeister CA. The relation between the composition of certain ternary two-phase solvent systems and RM values. J. Chromatogr. 1962; 7:311–320.

(47). Snyder LR, Dolan JW, Gant JR. Gradient elution in high-performance liquid chromatography. I. Theoretical basis for reversed-phase systems. J. Chromatogr. 1979; 165:3–30.

(48). Frisch, MJ.; Trucks, GW.; Schlegel, HB.; Scuseria, GE.; Robb, MA.; Cheeseman, JR.; Scalmani, G.; Barone, V.; Mennucci, B.; Petersson, GA.; Nakatsuji, H.; Caricato, M.; Li, X.; Hratchian, HP.; Izmaylov, AF.; Bloino, J.; Zheng, G.; Sonnenberg, JL.; Hada, M.; Ehara, M.; Toyota, K.; Fukuda, R.; Hasegawa, J.; Ishida, M.; Nakajima, T.; Honda, Y.; Kitao, O.; Nakai, H.; Vreven, T.; Montgomery, JA., Jr.; Peralta, JE.; Ogliaro, F.; Bearpark, M.; Heyd, JJ.; Brothers, E.; Kudin, KN.; Staroverov, VN.; Kobayashi, R.; Normand, J.; Raghavachari, K.; Rendell, A.; Burant, JC.; Iyengar, SS.; Tomasi, J.; Cossi, M.; Rega, N.; Millam, JM.; Klene, M.; Knox, JE.; Cross, JB.; Bakken, V.; Adamo, C.; Jaramillo, J.; Gomperts, R.; Stratmann, RE.; Yazyev, O.; Austin, AJ.; Cammi, R.; Pomelli, C.; Ochterski, JW.; Martin, RL.; Morokuma, K.; Zakrzewski, VG.; Voth, GA.; Salvador, P.; Dannenberg, JJ.; Dapprich, S.; Daniels, AD.; Farkas, O.; Foresman, JB.; Ortiz, JV.; Cioslowski, J.; Fox, DJ. *Gaussian 09*, revision A.02. Gaussian, Inc.; Wallingford, CT: 2009.

(49). Chai JD, Head-Gordon M. Systematic optimization of long-range corrected hybrid density functionals. J. Chem. Phys. 2008; 128:084106-1–084106-15. [PubMed: 18315032]

(50). Weigend F, Ahlrichs R. Balanced basis sets of split valence, triple zeta valence and quadruple zeta valence quality for H to Rn: design and assessment of accuracy. Phys. Chem. Chem. Phys. 2005; 7:3297–3305. [PubMed: 16240044]

(51). Andrae D, Haeussermann U, Dolg M, Stoll H, Preuss H. Energy-adjusted ab initio pseudopotentials for the second and third row transition elements. Theor. Chim. Acta. 1990; 77:123–141.

(52). Miertuš S, Scrocco E, Tomasi J. Electrostatic interaction of a solute with a continuum. A direct utilization of ab initio molecular potentials for the prevision of solvent effects. Chem. Phys. 1981; 55:117–129.

(53). Foresman JB, Keith TA, Wiberg KB, Snoonian J, Frisch MJ. Solvent effects 5. The influence of cavity shape, truncation of electrostatics, and electron correlation on ab initio reaction field calculations. J. Phys. Chem. 1996; 100:16098–16104.

(54). Reed AE, Weinstock RB, Weinhold F. Natural-population analysis. J. Chem. Phys. 1985; 83:735–746.

Europe PMC Funders Author Manuscripts

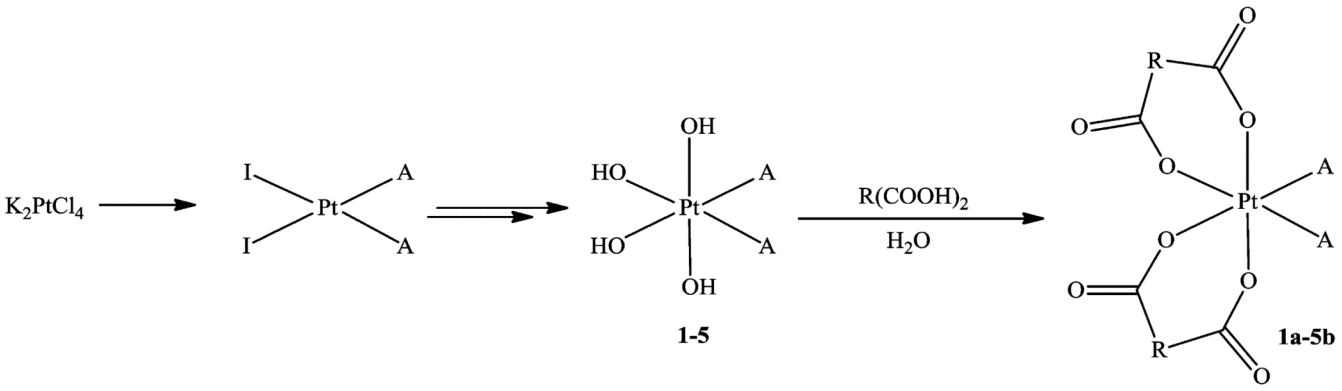

Figure 1.

Synthesis of novel diam(m)inebis(dicarboxylato)platinum(IV) complexes of the type Pt(diam(m)ine)($R(COO)_2)_2$: A = NH_3, $EtNH_2$, or cha (cyclohexylamine) or A_2 = en (ethane-1,2-diamine) or DACH ((1*R*,2*R*)-diaminocyclohexane); $R(COOH)_2$ = oxalic, malonic, 3-methylmalonic, or 1,1-cyclobutanedicarboxylic acid.

Europe PMC Funders Author Manuscripts

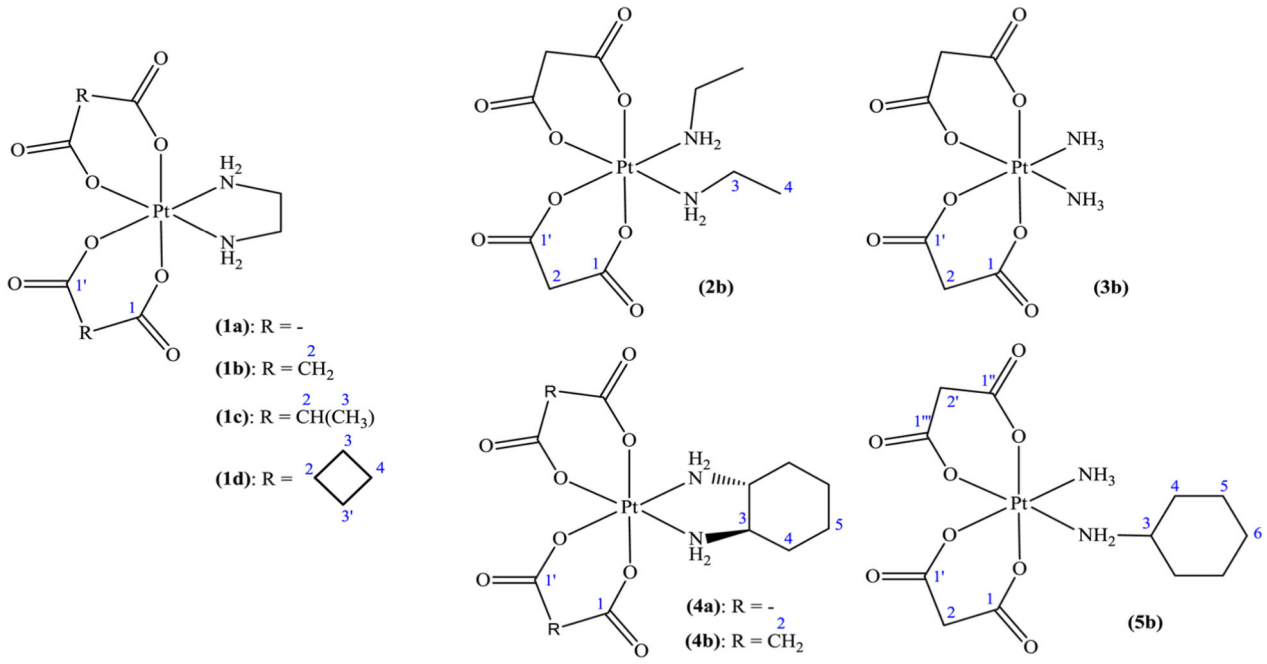

Figure 2.
Chemical structures of novel diam(m)inebis(dicarboxylato)platinum(IV) complexes along with their NMR numbering schemes.

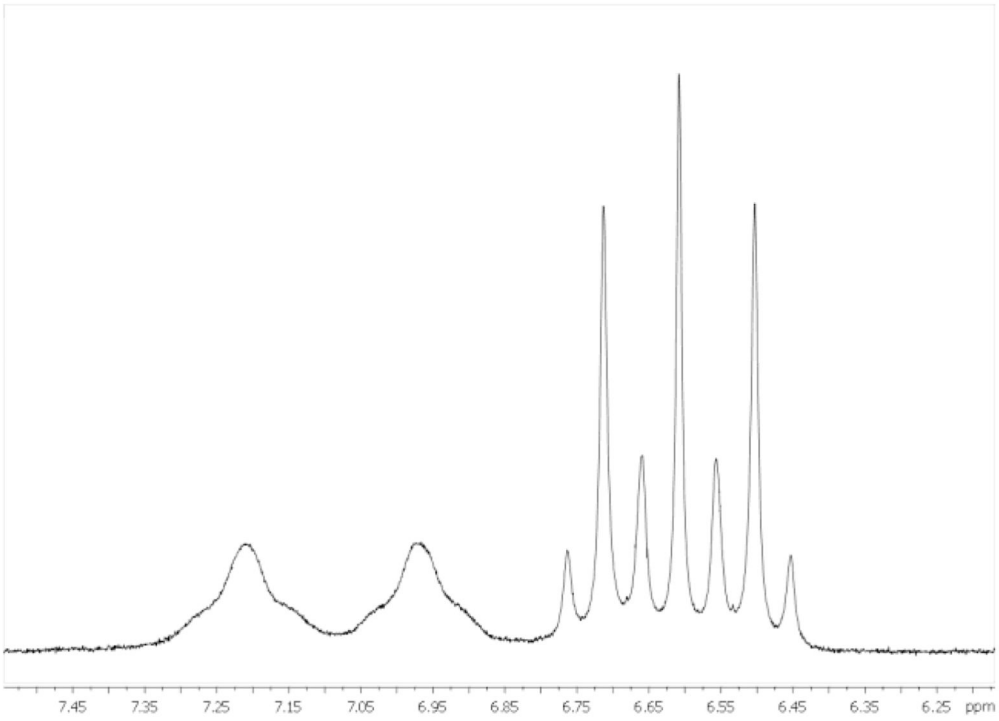

Figure 3.

NH_2 (left) and NH_3 (right; $^1J_{N,H}$ = 52.6 Hz, $^2J_{Pt,H}$ = 51.4 Hz) signals of complex **5b** in the ^1H NMR spectrum.

Europe PMC Funders Author Manuscripts

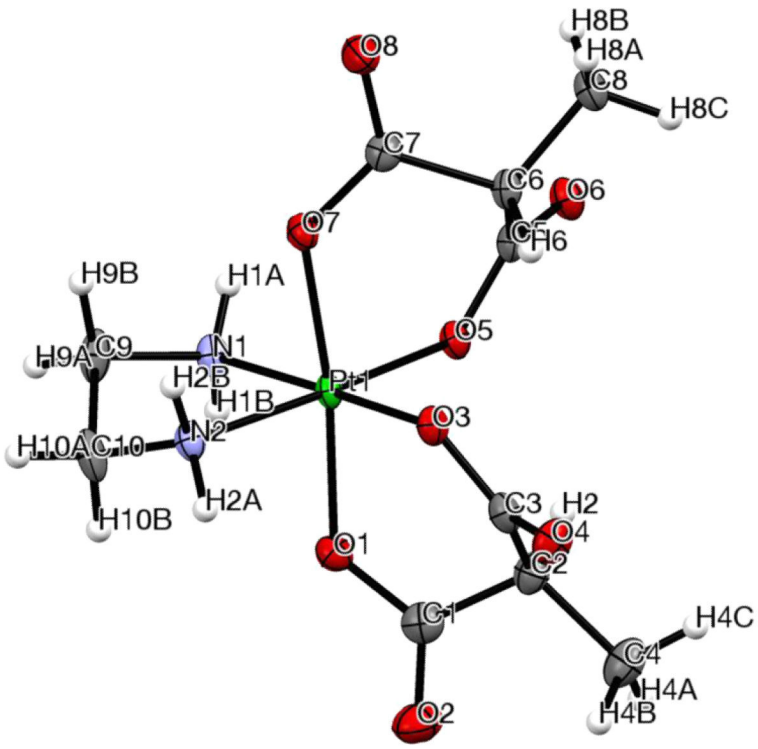

Figure 4.

ORTEP view of complex **1c** with its atom labeling scheme. The thermal ellipsoids are drawn at the 50% probability level. Selected bond lengths (Å) and bond angles (deg): Pt–N1 2.023(3), Pt–N2 2.024(2), Pt–O1 1.988(2), Pt–O3 2.016(2), Pt–O5 2.020(2), Pt–O7 1.988(2), N1–Pt–N2 84.65(10), O3–Pt–O5 96.83(8), N1–Pt–O5 88.45(9), N2–Pt–O3 90.10(9), O1–Pt–O3 92.54(10), O5–Pt–O7 93.22(9), O1–Pt–O7 172.54(9).

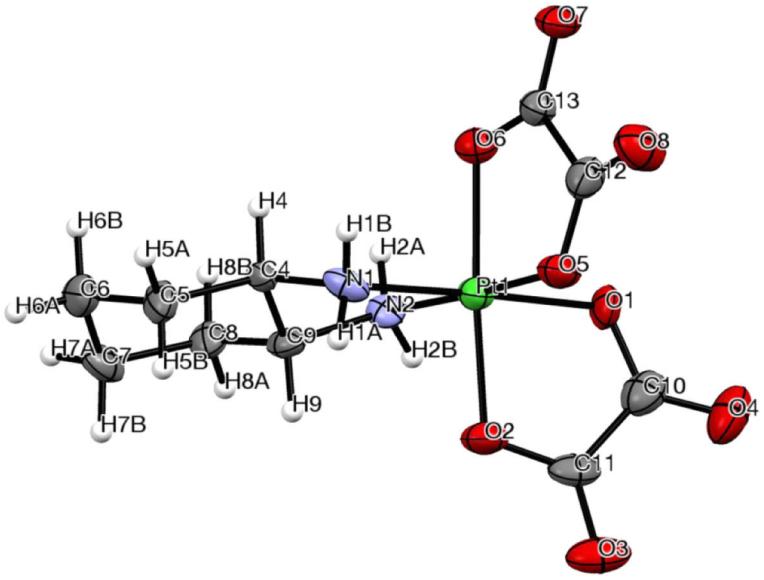

Figure 5.

ORTEP view of complex **4a** with its atom labeling scheme. The thermal ellipsoids are drawn at the 50% probability level. Selected bond lengths (Å) and bond angles (deg): Pt–N1 2.029(10), Pt–N2 2.032(8), Pt–O1 2.027(8), Pt–O2 1.999(8), Pt–O5 1.993(8), Pt–O6 2.028(8), N1–Pt–N2 84.3(4), O1–Pt–O5 87.0(3), N1–Pt–O5 93.1(4), N2–Pt–O1 95.6(3), O1–Pt–O2 84.6(3), O5–Pt–O6 84.7(3), O2–Pt–O6 176.3(3).

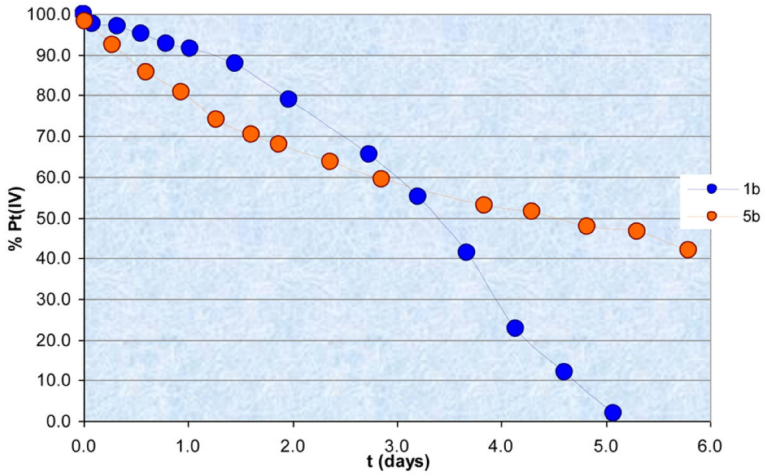

Figure 6.

Time-dependent reduction of **1b*** and **5b*** (2 mM) in the presence of sodium ascorbate (30 mM) at ambient temperature.

Europe PMC Funders Author Manuscripts

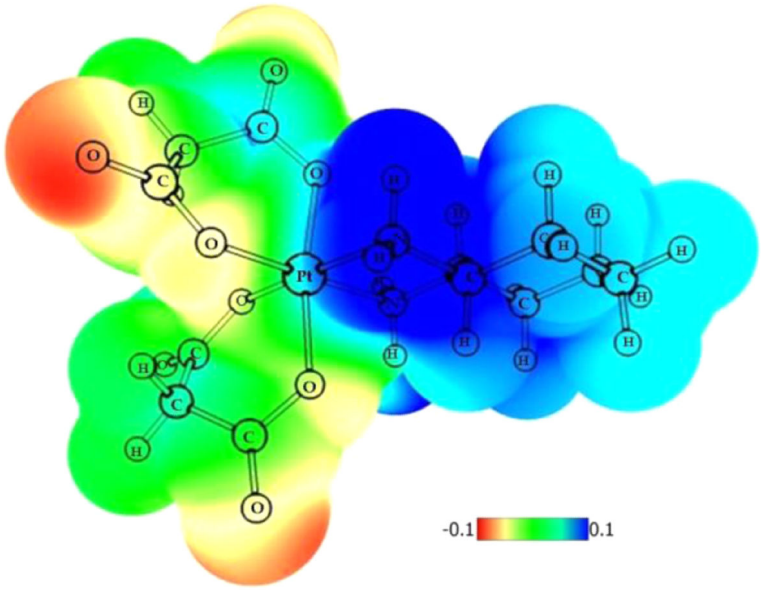

Figure 7.
ESP color-mapped electron density for complex **4b**.

Europe PMC Funders Author Manuscripts

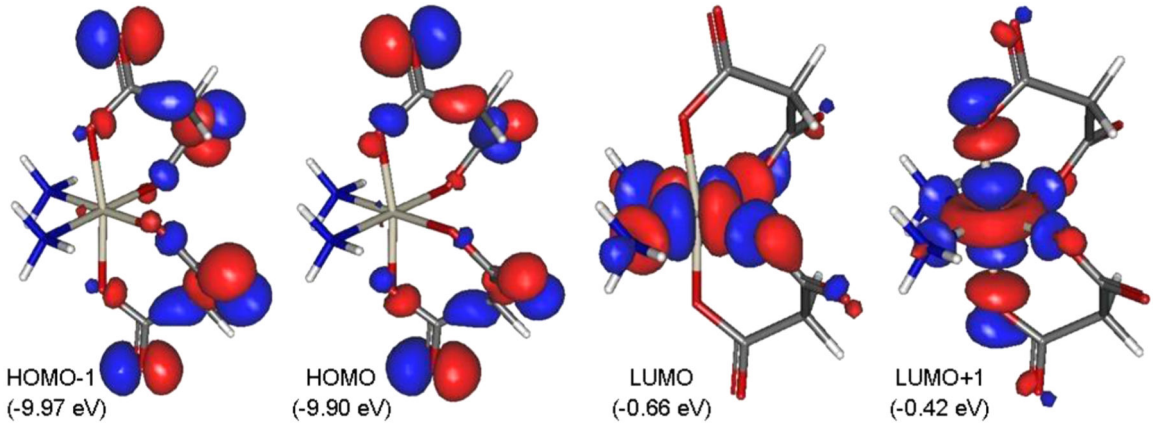

Figure 8.
Frontier orbitals (with their energies) of complex **3b**.

Europe PMC Funders Author Manuscripts

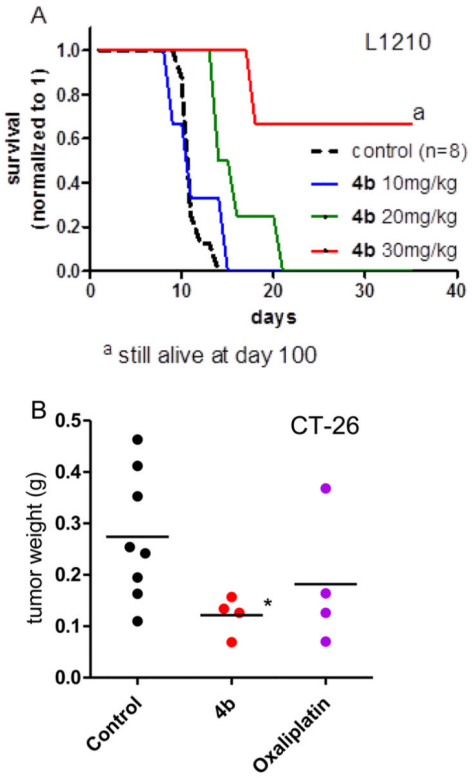

Figure 9.

Anticancer activity of **4b** in vivo: (A) Kaplan–Meier plots showing the survival (days after tumor implantation) of L1210 leukemia-bearing mice treated intraperitoneally with the indicated doses of **4b** (n = 4) on days 1, 5, and 9 compared to that of solvent-treated controls (n = 8). (B) CT-26 cells were injected subcutaneously into the right flank of BALB/c mice. Mice were treated on days 4, 7, 11, and 14 with 30 mg/kg (i.p.) of **4b** or 9 mg/kg (i.v.; maximal tolerated dose) of oxaliplatin. Animals were sacrificed on day 15, and tumors were collected. Statistical analysis was performed by Student's t test (* $p < 0.05$ compared to control mice).

Europe PMC Funders Author Manuscripts

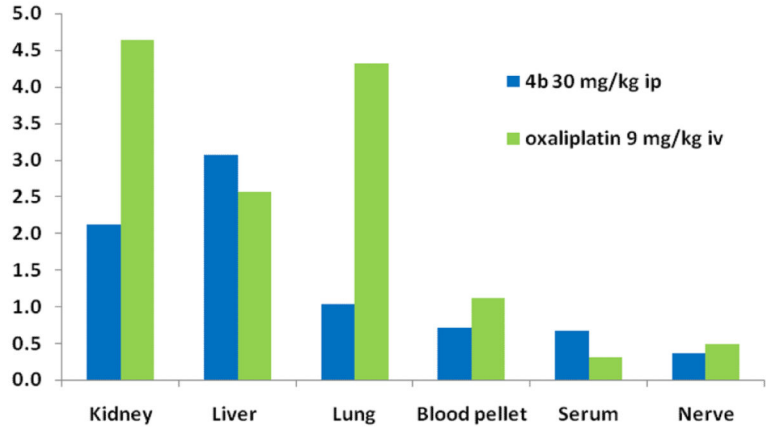

Figure 10.

Platinum accumulation in mouse tissues, blood pellet, and serum collected on day 15 from the CT-26 experiment shown in Figure 9B; values are normalized relative to the platinum content found in the tumor (~5 μg/g for **4b** and ~1 μg/g for oxaliplatin, respectively). Mice were treated on days 4, 7, 11, and 14 with 30 mg/kg of **4b** (intraperitoneal, ip) or 9 mg/kg of oxaliplatin (intravenous, iv).

Europe PMC Funders Author Manuscripts

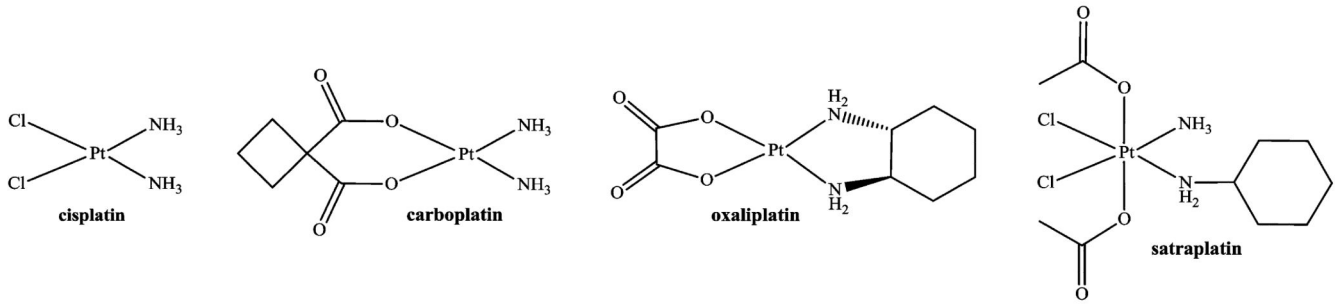

Scheme 1. Chemical Structures of Platinum(II) Complexes with Worldwide Clinical Approval (Cisplatin, Carboplatin, and Oxaliplatin) and Platinum(IV)-Based Drug Candidate in Clinical Trials (Satraplatin)

Europe PMC Funders Author Manuscripts

Table 1

Log k_{30}[a] and Log k_w[b] for New Complexes as Well as for Carboplatin, Oxaliplatin, and Satraplatin

compd	log k_w	log k_{30}
1b	−0.63 ± 0.02[c]	−1.45 ± 0.13
1c	0.17 ± 0.02	−0.55 ± 0.02
1d	1.28 ± 0.01	0.28 ± 0.01
2b	0.18 ± 0.02	−0.62 ± 0.02
3b	−0.67 ± 0.01[c]	−1.54 ± 0.15
4a	−0.31 ± 0.02[c]	−0.80 ± 0.03
4b	−0.11 ± 0.01	−0.65 ± 0.02
5b	0.91 ± 0.01	0.01 ± 0.01
carboplatin	−0.36 ± 0.04[c]	−0.80 ± 0.01
oxaliplatin	0.17 ± 0.01	−0.82 ± 0.01
satraplatin	1.63 ± 0.04	0.68 ± 0.01

[a] Log *k*, obtained with a mobile phase containing 30% MeOH.

[b] Values extrapolated to 0% MeOH.

[c] Very hydrophilic compound; a lower accuracy of the extrapolated values can be expected because most of the measured log *k* values are below −0.5 and are therefore outside of the linearity range of the Soczewinski–Snyder relationship.[46,47]

Table 2

Cytotoxicity of Bis- and Tris-Chelate Diam(m)inebis(dicarboxylato)platinum(IV) Complexes in Three Human Cancer Cell Lines in Comparison with Several Clinically Relevant Platinum-Based Drugs[a]

		IC_{50}, 96 h[b]		
compd	**formula**	**A549**	**CH1**	**SW480**
1b	$Pt(en)(mal)_2$	>640	80 ± 20	>640
1c	$Pt(en)(memal)_2$	>200	202 ± 5	>200
1d	$Pt(en)(CBDCA)_2$	>640	170 ± 54	>640
2b	$Pt(EtNH_2)_2(mal)_2$	>200	222 ± 14	>200
3b	$Pt(NH_3)_2(mal)_2$	>200	32 ± 9	>200
4a	$Pt(DACH)(ox)_2$	46 ± 7	4.1 ± 0.9	14 ± 3
4b	$Pt(DACH)(mal)_2$	257 ± 70	19 ±4	26 ± 6
5b	$Pt(NH_3)(cha)(mal)_2$	>200	18 ± 3	165 ± 40
satraplatin	$Pt(NH_3)(cha)Cl_2(OAc)_2$	6.4 ± 0.4	0.10 ± 0.02	1.5 ± 0.1
cisplatin	$Pt(NH_3)_2Cl_2$	6.2 ± 1.2	0.077 ± 0.006	3.3 ± 0.2
carboplatin	$Pt(NH_3)_2(CBDCA)$	91 ± 10[c]	0.81 ± 0.17	37 ± 1
oxaliplatin[d]	Pt(DACH)(ox)	0.98 ± 0.21	0.18 ± 0.01	0.29 ± 0.05

[a] See Scheme 1 for chemical structures.

[b] 50% inhibitory concentrations (means ± standard deviations from at least three independent experiments), as obtained by the MTT assay using an exposure time of 96 h.

[c] Data taken from ref 26.

[d] Data taken from ref 35.

Table 3

Calculated Physicochemical Parameters for the Investigated Complexes[a]

compd	V_m (cm^3/mol)	μ (D)	α (bohr^3)	SASA (bohr^2)	E_s (kJ/mol)	E_{HOMO} (eV)	E_{red} (eV)
1a	151	16.6	132	868	177	−9.74	4.13
1b	170	12.7	153	1021	148	−9.78	3.97
1c	199	12.2	176	1051	145	−9.80	3.98
1d	229	12.0	210	1282	140	−9.57	3.92
2b	235	11.4	180	1067	132	−9.74	3.96
3b	156	10.5	135	906	151	−9.90	3.95
4a_1	195	18.4	174	1031	168	−9.62	4.15
4a_2	206	18.4	174	1054	168	−9.62	4.11
4b_1	214	14.4	196	1133	139	−9.67	3.96
4b_2	209	14.4	195	1140	140	−9.67	3.95
5b	221	11.8	199	1219	128	−9.79	4.00

[a]Molar volume (V_m), dipole moment (μ), polarizability (α), solvent-accessible surface area (SASA), adiabatic energy of hydration (E_S), energy of HOMO (E_{HOMO}), and adiabatic electron affinity in water (E_{red}).